Republic of Iraq
Ministry of Higher Education and Scientific Research
University of Al-Nahrain
College of Sciences

DESIGN OF PHOTONIC CRYSTAL FIBER SENSOR

A Thesis Submitted to the College of Sciences – Alnahrain University as a Partial Fulfillment of the Requirements for the Degree of Master of Science in Physics

By

Soror Ali Mahdi Al-Khafaji

(B.Sc. 2013)

Supervisor

Ass.Prof. Suha Mousa Khorsheed

2016 A.D. *1437 A.H.*

﴿يَرْفَعِ اللَّهُ الَّذِينَ آمَنُوا مِنْكُمْ
وَالَّذِينَ أُوتُوا الْعِلْمَ دَرَجَاتٍ وَاللَّهُ
بِمَا تَعْمَلُونَ خَبِيرٌ﴾

سورة المجادلة الآية ١١

Supervisor Certification

We certify that this thesis entitled **"Design of a Photonic crystal fibers sensor"** under our supervision at College of Science / Al-Nahrian University as a partial fulfillment of requirements for the Degree of Master of Science in Physics.

Signature:
Name: **Dr.Suha Mousa Khorsheed**
Scientific Degree**:** Assistant Professor
Date: / /2016

In view of the available recommendations, I forward this thesis for debate by the Examination Committee.

Signature:
Name: **Dr.Alaa Jabbar Ghazai**
Scientific Degree**:** Assistant Professor
Tittle: Head of the department of Physics
College of Science / Al-Nahrian University.
Date: / /2016

Committee Certification

We, the examining committee certify that we have read this thesis entitled **" Design of a Photonic crystal fibers sensor "** and examined the student "**Soror Ali Mahdi**" in its contents and that in our opinion , it is accepted for the Degree of Master of Science in Physics.

Signature:
Name:**Dr.Hayfa G.Rashid**
Scientific Degree:Professor
Date: / /2016
(Chairman)

Signature:
Name: **Dr.Kamal H.Lateef**
Scientific Degree: professor
Date: / /2016
(Member)

Signature:
Name: **Dr.Alaa Jabbar Ghazai**
ScientificDegree:Assistant
Date: / /2016
(Member)

Signature:
Name: **Dr.Suha Mousa Khorsheed**
Scientific Degree: Assistant professor
Date: / /2016
(Member/ Supervised)

-

I, hereby certify upon the decision of the examining committee.

Signature:
Name: **Dr. Hadi M. A. Abood**
Title: Assistant Professor
Address: Dean of the College of Science
Date: / /2016

الأهداء

الى القلب الناصع بالبياض .... **أمي**

الى من أحمل أسمك بكل فخر .... **أبي**

الى الروح التي سكنت روحي .... **زوجي**

الى سندي وقوتي وملاذي .... **أخوتي**

الى من تذوقت معهم اجمل اللحظات .... **أصدقائي**

الى من مهدوا لي طريق العلم والمعرفة .... **أساتذتي**

وإلى كل من ساندني أهدي هذا البحث راجية من المولى

عز وجل أن يجد القبول والنجاح

Acknowledgments

*First of all, thank to **ALLAH** for every think*

I would like to acknowledge my sincere thanks and appreciation to my supervisor Dr. Suha Mousa Khorsheed for suggesting the project, assistance, encouragement, valuable advice, for giving me the major steps to go on to explore the subject, sharing with me the ideas in my research "DESIGN OF PHOTONIC CRYSTAL FIBERS SENSOR", and discuss the points that I left they are important.

Grateful Thanks are due to Dr. Ahmad K. Ahmad and Dr. Hussain Thamer for their advices to me during the research period. Also, I would like to thanks Dr.Nesreen and Alaa Adnan for introducing the help to me along the time of the practical work.

Many thanks expressed to the Head of Physics Department, and the staff of the Department for their kind attention.

Sincere thanks to my father for his efforts, and family for their help and patience, and thanks to my faithful friends for supporting and giving me advises.

Soror

2016

List of Contents

List of Figures

List of Tables

List of symbols and abbreviation

PCF	Photonic crystal fiber.
LC	Liquid crystal.
EBBA	N-(4`-ethoxybenzylidene)-4-n-butylaniline liquid crystal.
FTIR	Fourier transforms infrared spectroscopy.
LMA	Large mode area.
HC	Hollow core.
TIR	Total internal reflection.
PBG	Photonic bandgap.
$\mathbf{n_{core}}$	Core refractive index.
$\mathbf{n_{cladding}}$	Cladding refractive index.
IGPCF	Index guiding photonic crystal fiber.
PBGF	Photonic bandgap fiber
CL	Confinement loss.
A	Attenuation constant.
SMF	Single mode fiber.
NLC	Nematic liquid crystal.
CLC	Cholesteric liquid crystal.
$\mathbf{P_i}$	Input power.
$\mathbf{P_o}$	Output power.
CL	Confinement loss.
n	Nematic.
i	Isotropic.
OSA	Optical spectrum analyzer

Abstract

The present work aims to employ the photonic crystal fiber (PCF) for designing temperature and electric field sensors with intended manufacturing characteristics including: high sensitivity, repeatability and low cost by infiltrated with Nematic N-(4`-ethoxybenzylidene)-4-n-butylaniline liquid crystal(EBBA) liquid crystal. The novelty in this work is the use of EBBA that characterized by its ability to align by an external electric field. Aligned EBBA have the optical properties of uniaxial crystal, which makes it candidate to be useful in different applications

The proposed temperature and electric field sensor are designed and implemented, the process of the design is requires passing through two work stages: they are, liquid crystal preparation and sensors design. The liquid crystal preparation phase is responsible on preparing the EBBA using its chemical components to be injected in the PCF in the following work stages. EBBA was identified using Fourier transform infrared spectroscopy (FTIR) at transition temperature range between 36-80 ℃. Then, EBBA was used to measure the values of refractive index at temperature range 25-80℃. The result showed that the values of refractive index decreases with increasing the temperature. Later, EBBA was used in the following sensors design phase. Whereas, the sensor design phase is responsible on constructing the sensor components and setting them according to the proposed design.

The implementation of the temperature sensor was carried out by splicing short lengths of large mode erea (LMA-10) PCF with conventional single mode fiber (SMF-28) in one side and using free space connector from other side. A diode laser of different wavelengths (1550, 1060, 850 *nm*) and helium-neon laser of 632.8 *nm* has been used as a light source, where a high sensitive optical spectrum analyzer (OSA) was used to monitor and record the transmitted spectra. Whereas, the implementation of the electric field sensor was carried out by using short length of hollow core (HC-1550) PCF. A diode laser was used of wavelength

equal to 650 *nm* has been used as a light source for guiding the light to the one side of the fiber, the other side infiltration with EBBA liquid crystal by capillary effect. Then, record the transmission a spectrum is recorded by using the fiber optic spectrometer.

The proposed sensors are used in the next testing stage. The test includes infiltrating the air holes of the PCFs by liquid crystal instead of air. For temperature sensing, the EBBA liquid crystal material was prepared to infiltrate the air holes for the solid core (LMA-10) PCF, which leads to change the refractive index of the PCF and affects the transmission of the laser inside the PCF due to the change happen in the value of the refractive index of the liquid crystal. The results showed that the power of transmission spectrum after PCF infiltration will be increased with increasing temperature. The value of sensitivity can be achieved by the slope of the line for the figure of transmission and temperature. The highest sensitivity has been obtained that reached 0.02 $dBm/^{o}C$ at 1550 *nm* with less loss and less attenuation. For electric field sensing, the EBBA liquid crystal infiltrate the air holes for the hollow core (HC-1550) PCF. The infiltrated section of photonic crystal fiber was equal to ~1 *cm*. The results show that the power of transmission spectrum will be remains unchanged until reach the electric field intensity to 97.2 *Vrms/mm*. Implies the region of the electric field sensor operating is between (97.2 *Vrms/mm* to 146.8 *Vrms/mm*).After this region, there is no change may happen in the electric field. The sensitivity can be finding by the slope of transmission and electric field intensity. It was found that the intensity of the proposed electric field sensor was 0.00123 *dBm.mm/Vrms* at 650 *nm*.the achieved sensitivity values were acceptable in comparison with that mentioned in latretures,this ensure the correct results and methodology.

CHAPTER ONE

INTRODUCTION AND LITERATURE REVIEW

CHAPTER ONE

INTRODUCTION AND LITERATURE REVIEW

1.1 Introduction

Optical fiber is used every day in our daily lives in the connecting to the internet, making telephone calls and reading our e-mails. Different applications in optical communication networks were performed using photonic crystal fiber, such as: spectroscopy, astronomy, biomedical imaging, diagnostic, and structural sensing. One of the important applications is still the physical sensors, which are: temperature sensor, magnetic field sensor, and electric field sensor [1].

An optical fiber is a cylindrical dielectric waveguide that transmits light along its axis, by the process of total internal reflection. The fiber consists of a core surrounded by a cladding layer, both of them are made of dielectric materials. To confine the optical signal in the core, the refractive index of the core must be greater than that of the cladding. Conventional optical fibers are formed from two different type of silica. The middle of the fiber is forming the core of the fiber with higher refractive index, whereas the second part is forming the glad of optical fiber and surrounds the core with refractive index that should be lower than the core as shown in Figure (1.1) [2].

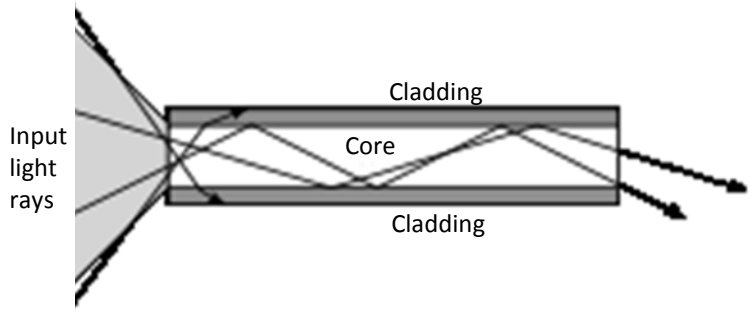

Fig (1.1) Conventional photonic crystal fibers [2].

The major difference between two kinds of fibers: conventional optical fiber and photonic crystal fiber based on the fact that the waveguide properties of photonic crystal fibers are not from spatially varying glass composition, as in conventional optical fiber, but from an arrangement of air holes which go through the whole length of fiber. In contrast with conventional optical fibers, photonic crystal fiber can be made of a single material and have several geometric parameters which can be manipulated offering large flexibility of design, and more these fibers offer also the possibility of light guiding in a hollow core, opening new perspectives in fields such as nonlinear fiber optics, fiber laser, particle guidance and fiber sensors [3, 4].

1.2 Photonic Crystal Fiber

Photonic crystal fiber (PCF) is also called holey fiber or microstructure optical fiber that was firstly reported by Philip Russell [5]. This new generation of optical fiber was appeared in mid 1990s to investigate the idea of making PCF from single material [6].

Photonic crystal fiber are made from a single material such as silica glass with periodic arrangement of air holes lies along the length of the fiber, with the scale of micro structuring being comparable to the wavelength of the electromagnetic radiation guided by the fibers. The light is confined in solid core by exploiting the modified total internal reflection, so the photonic crystal fibers of non-filling holes are more similar to conventional optical fibers, where the difference of refractive index between the core region and the gladding region is positive, because the refractive index of air-holes is lower than the refractive index of the core [7].

There are two types of photonic crystal fibers: solid core PCFs and hollow core PCF. The solid core with cross-section presents a periodic array of air holes surrounding a solid core, which are extended invariantly along the fiber length.

The second one is the hollow core photonic crystal fibers, which means an air-silica gladding surrounding a hollow core [8].

Therefore, photonic crystal fibers can be categorized in two types depend on its material: it is may be solid-core photonic crystal fiber or hollow-core photonic crystal fibers. Therefore, different geometry and different materials will present different structural design used to enable different guidance mechanisms in photonic crystal fibers. These guidance mechanisms are: modified total internal reflection and photonic bandgap guidance. Such that, there are four different guidance mechanisms are found depending on the geometry and core/gladding materials of photonic crystal fiber; they are [4]:

(i) index-guiding PCF, which used to guides in a solid core through modified total internal reflection.
(ii) Photonic bandgap-guiding PCF, which used guides through photonic bandgap effect in a hollow-core.
(iii) all-solid photonic bandgap PCF, which used to introduce guidance through photonic bandgap anti-resonant effect in a solid core.
(iv) Hybrid PCF, which used to introduce guidance through simultaneous propagation of photonic bandgap and modified total internal reflection.

In the solid core PCF, the effective refractive index of the gladding will be lowered when with the refractive index of the core, allowing the guidance mechanism to be total internal reflection, without need to dope the core, allowing the solid core PCFs to be made with a single material. Whereas, the hollow PCF confines the light by the bandgap mechanism, which based on the photonic bandgap effect [8]. Also, the PCFs can be divided into two groups depending on the geometry of arranging holes along the cross section of the photonic crystal fiber: the first is called index guiding photonic crystal fiber (IG PCFs) while the second group is called and photonic band gap fibers (PBGFs), as in Figure (1.2) shows [9].

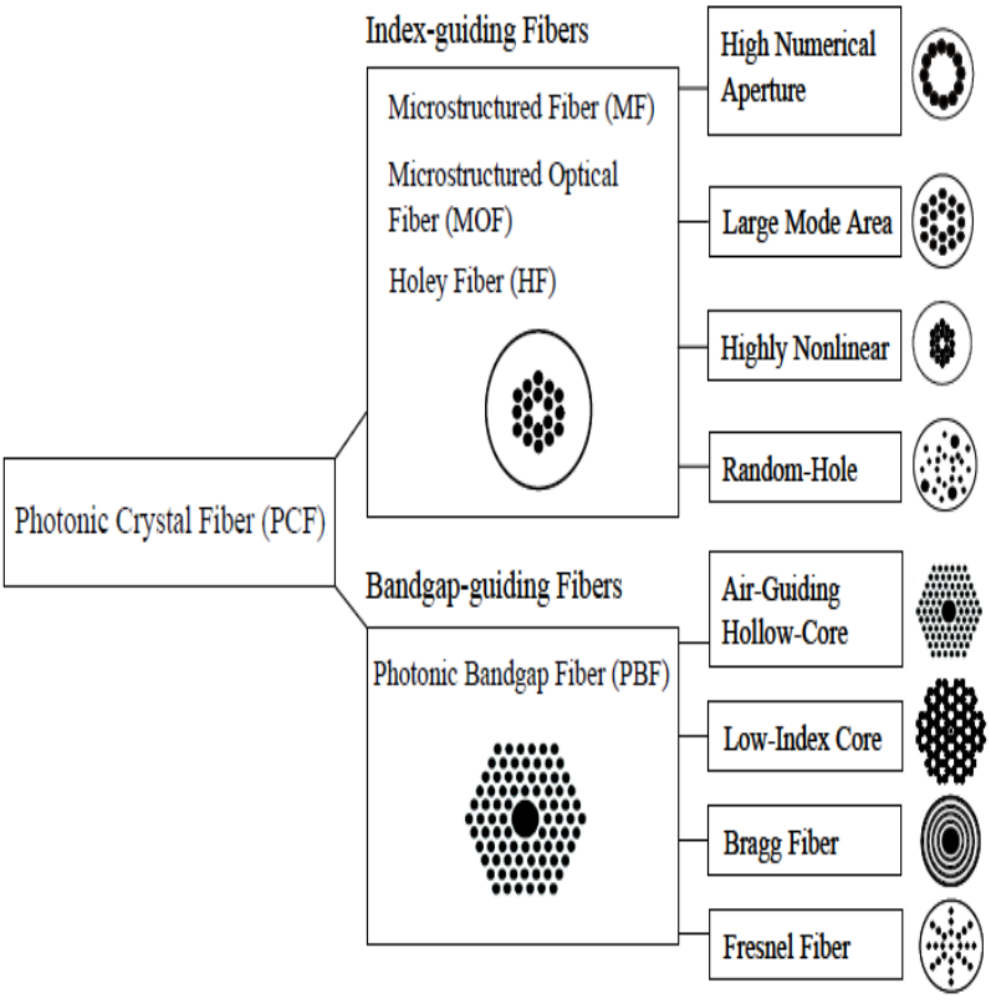

Fig (1.2) Categorization of photonic crystal fibers [9].

1.3 Photonic Liquid Crystal

A photonic liquid crystal is a periodic optical nanostructure that affects the motion of photons in much the same way that ionic lattices affect electrons in solids. Photonic crystals occur in nature in the form of structural coloration, which promise to be useful in a range of applications. It shows the intermediate phases represent a new thermodynamic state of matter that are quite distinct from the isotropic liquid. The mechanical and symmetry properties of these phases are

intermediate between those of a crystalline solid and an isotropic liquid. Lehmann first referred to them as flowing crystals and later used the term "liquid crystals phases" are also called mesophases and liquid crystal molecules are called mesogens [10]

The distinguishing characteristic of the liquid crystalline state is the tendency of mesogens to point along a common axis called the director (n) which is a unit vector and is called the liquid crystal director. In the solid state, molecules are highly ordered and have little translational freedom. The characteristic orientation order of the liquid crystal state is between the solid and liquid phases [11]. The alignment of the molecules for each phase is shown in the Figure (1.3).

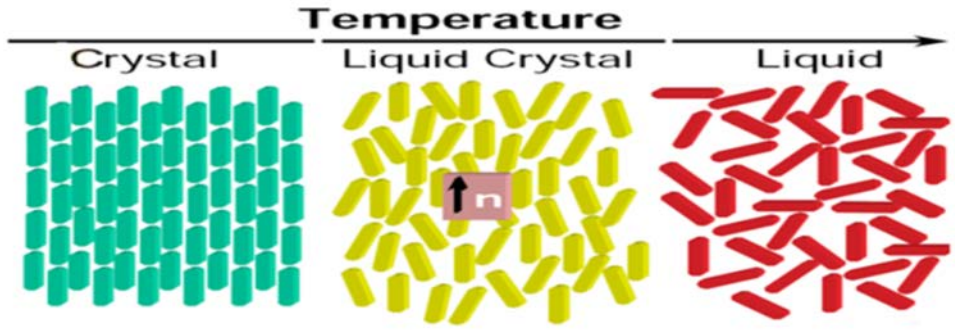

Fig (1.3) Alignment of molecules for solid, liquid crystal and liquid phases [11].

The physical properties of such liquid crystal are distinguished into scalar and nonscaler properties. Typical scalar properties are the thermodynamic (transition density and fractional density change). The dielectric diamagnetic, optical, elastic and viscous coefficients are the important nonscalar properties .

The transition temperatures and transition densities are the important quantities characterizing the materials. The difference in the transition temperature between the melting and clearing point gives the range of stability of the liquid crystalline phases [12].

1.4 Literature Review

There are a great deal of focus was granted to photonic crystal fiber sensors. Numerous approaches were developed in order to achieve the more efficient technique to serve the wide applications of field of interest. In the following, the most significant literatures are mentioned in details:

1. T.R Wolinsk et al (2006)[13],demonstrated the electric field and temperature effect on the propagation of the photonic liquid crystal fiber composed of solid-core PCF filled with a prototype NLC or with typical nematic pentylo-cyano-biphenyl(PCB).
2. Jian Ju et al (2006)[14],investigated theoretically and experimentally of the temperature sensitivity through two-mode(TM) photonic crystal fiber(PCF) sensor, and was measured the temperature sensitivity and found equal to 0.083 rad/℃.m at 543 nm and 0.147 rad/℃.m at 975 nm and 0.136 rad/℃.m at 1310 nm.
3. O.Frazao et al (2007) [15],demonstrated the temperature insensitive and strain sensor by using Hi-Bi photonic crystal fiber loop mirror.the optical sensor was characterizedin temperature and strain with coated Hi-Bi photonic crystal fiber and uncoated Hi-Bi photonic crystal fiber , the optical sensor is insensitive to temperature(0.9 pm/k).
4. T.R Wolinsk et al (2008)[16],presented experimental results showing the influence of temperature and external electric field and hydrostatic pressure on the propagation properties of the photonic crystal fibers infiltrated with liquid crystal with low and medium material anisotropies. Give information about the value of temperature, voltage, and pressure by measured induced shifts of the photonic bandgap wavelengths.
5. L.Viet Nguyen et al (2008) [17], presented interference pattern by using the multimode-single mode-multimode (MM-SM-MM) fiber configuration and applied to demonstrated the temperature fiber sensor. The result shown the

temperature sensitivity equal 0.088 nm/℃ and can be measure at high temperature stably up to 900℃.

6. Y.Yu et al (2010) [18], introduced the temperature sensor photonic crystal fiber based on intensity modulation and filling the air holes by liquid ethanol. The confinement loss and effective refractive index of the PCF became high temperature-dependent because the thermo-optic coefficient of liquid ethanol used is high compared with silica dioxide and this temperature dependence increasing function of d/Λ ratio and the input wavelength.the result shown the temperature sensitivity of the sensors equal to 0.35 dB/℃ for 10 cm long of photonic crystal fiber.
7. S.Mathews et al(2011)[19],demonstrated and evaluated the directional sensitivity of maintaining photonic crystal fiber(PM PCF) in an electric field for sensing of electric field and showing that the sensor probe has higher sensitivity to the electric field component aligned along the Hi-Bi PCF axis.
8. S.Mathews et al(2011)[20],studied the intensity measurement based electric field sensor by infiltrating an LMA PLC with an liquid crystal(MDA-2782) infiltrated section <1cm , and demonstrated the sensitivity in transmission is ~10.1db per kv_{rms} /mm and in reflection is ~4.55 db per kv_{rms} /mm.
9. A.Bozolan et al (2012) [21], demonstrated the optical fiber temperature sensor based on colloidal quantum dot luminescence. The result show the temperature sensitivity equal to 70 pm/℃ spectral shift over the range from 5℃ to 90℃.
10. L.Rindorf and O.Bang(2013) [22],studied the sensitivity of fiber grating sensors in the application of temperature, strain, bio sensing, and refractive index sensing.after infiltrated samples in photonic crystal fibers and for temperature and strain index sensing shown that the sensitivity is almost constant for all photonic crystal fibers and equal ~5 pm/k of photonic crystal fiber grating at low temperature.
11. Ashwini.M et al (2013) [23], studied the temperature property of gratings in photonic crystal fiber and analyzed the relationship between frequency shift, wavelength shift, effective index and temperature by finite difference time

domain method. The result show that the PCF gratings are in proportion to the temperature and thus applicable as temperature sensor.

12. Ran Wang et al (2013)[24],demonstrated the sensor probe for temperature measurement by using reflective photonic crystal fiber(LMA-8 PCF).the experimental result show that the reflected power exhibits a linear response with temperature with sensitivity equal to 1db/℃,and the emperature sensitivity with mixture of liquids is about 0.75 db/℃.
13. J.E.Antoni-Lopez et al (2014)[25],demonstrated the temperature sensitivity by using customized multicore fiber (MCF),measured temperature sensitivity with high sensitivity and accuracy and found the sensitivity equal 29pm/℃ at lower temperatures and increasing temperature up to 1000℃ and found the temperature sensitivity equal 52 pm/℃.
14. M.M.Tefelska et al (2014)[26],described four different types of micro-electrodes systems for electric field sensing with photonic crystal fibers infiltrated with liquid crystals. Also analyzed the capillary system theoretically, a capillary system with four micro electrodes (T~36ms) appeared to be the most convenient to operate with photonic liquid crystal fibers.
15. C.Markos et al (2015) [27], reported the fabrication and characterization of hybrid silica photonic crystal fiber with integrated chalcogenide glass layer and shown how band gaps of the fiber can be thermally tuned. Temperature measurements indicated that the transmission windows can be tuned with a sensitivity as high as ~3.5 nm/℃.so the proposed fiber has potential for all fiber filtering and temperature sensing.
16. M.Ock Ko et al (2015)[28], proposed the electric field sensor by using cholesteric liquid crystal (CLC) Fabry-Perot etalon and broad band optical source. The transmitted or reflected wavelength from CLC Fabry-Perot etalon depends on the applied electric field. The valley wavelengths of the transmitted light from CLC device are linearly increased from 1303 nm to 1317 nm as the applied electric field to the CLC device is increased from 0.8 V/μm to 1.9 V/μm.

1.5 Aim of Thesis

The present work aims to prepare photonic crystal fiber. Then, the prepared photonic crystal fiber is used to design a photonic crystal fiber sensor sensitivly to the temperature and electric field. Such sensor is operating on large mode area of photonic crystal fiber (LMA-10 PCF), (HC-1550 PCF) and EBBA liquid crystal. This requires passing through two stages are the preparation and design. The first stage includs preparing EBBA liquid crystal and determines its properties by changing the temperature using the ordinary refractive index of the liquid crystal. The second stage is designing a sensor is effective to the temperature and electric field.

1.6 Motivation of Thesis

The motivation we address in the present work is to obtain high performance sensors, in the sense of sensitivity, repeatability and low cost by infiltrated with Nematic EBBA liquid crystal. Nematics have fluidity similar to that of ordinary liquids but they can be easily aligned by an external magnetic or electric field. The novelty of the present work is the use of four wavelengths (632, 850, 1060, and 1550 *nm*) in the temperature sensor.

1.7 Thesis Layouts

The thesis consists of five chapters; chapter one is described thhe introduction to the basic concepts related to the photonic crystal fibers, whereas the other four chapters deal with the proposed sensor design method and discuss methodology for determining the efficiency of the sensor. Since Chapter Two introduces the concepts of photonic crystal fiber sensors. The theory of photonic crystal is explained with including the method of PCF sensor design. As well as, Chapter Three concerned with demonstrating stages and steps of the proposed design of the electrical and temperature sensor. The overall designing setup is described. Then, each stage and steps is explained mathematically with showing the related diagrams. In addition, Chapter Four shows the test results of applying

the proposed technique. The results are presented and discussed to evaluate the performance of establish sensor design. Finally Chapter Five contains some derived conclusions are listed and some suggestions for the future work are given.

CHAPTER TWO

THEORETICAL CONCEPTS

CHAPTER TWO
THEORETICAL CONCEPTS

2.1 Introduction

The principle of guiding the light by refraction makes fiber optics possible. The emerging field of photonic crystals led to the development in 1991 of photonic-crystal fiber, which guides light by diffraction from a periodic structure, rather than by total internal reflection. Latter, the first photonic crystal fibers became commercially available. Photonic crystal fibers can carry higher power than conventional fibers and their wavelength-dependent properties can be manipulated to improve performance [29].

There are many interesting materials for filling air-holes of PCF like alcohols, ethanol, liquid crystal, gas and biological materials. Infiltration of (LC) materials makes the susceptible to external field variations, this property which can be used to fabricate all fiber sensors for parameters such as temperature, magnetic fields and electric field [20]. Photonic crystal fiber has been widely used in telecommunication field, because the photonic bandgap fibers offer the possibility of low dispersion and low losses [30, 31]. The photonic bandgap fibers act as flexible system for atom optics. They can be filled with gasses or liquids, the interactions with liquids or gasses in air holes of both the fibers guides by PBG and the index guiding fibers show interesting potentials for sensing applications [32, 33]. Another applications used with photonic crystal fibers: high power fiber laser [34] and Raman scattering [35].

This chapter concerned with the study of types of fiber optics. The liquid crystal of type EBBA is discussed with details due to its importance in injecting the fiber cable. Moreover, the physical parameters such as: temperature, electric field, magnetic field, refractive index, that the physical sensor depending on, are briefly presented.

2.2. PCF Geometrical Characteristics

The geometric characteristics of fiber cross-section affect the behavior of PCF, such as: the core diameter (ρ), and the pitch (ʌ). The core diameter which for solid core PCF is defined as the diameter of the ring formed by innermost air holes, the pitch is the distance between the center of two consecutive air holes and the diameter of air holes of the gladding (d) as show in Figure (2.1). These physical parameters in combination with the type of lattice and the choice of the refractive index of the material make the fabrication of PCFs very flexible and open up the possibility to manage its properties, leading to freedom of design not possible with common fiber [7].

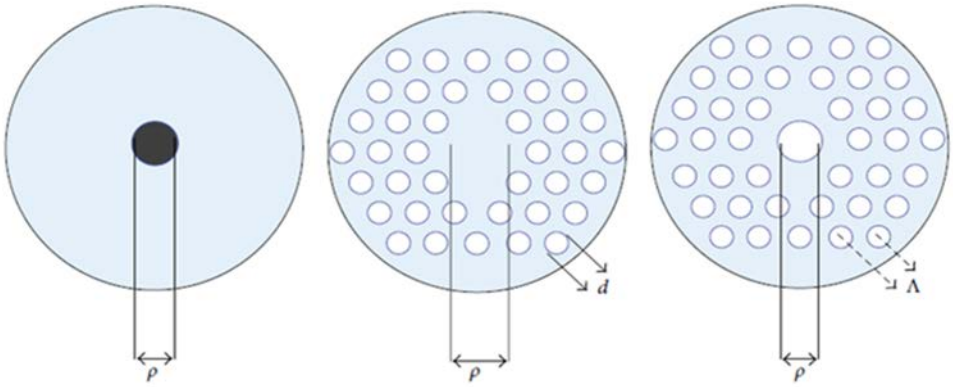

(a) SM fiber. (b) Solid core PCF. (c) Hollow core PCF.

Fig (2.1) Cross section of different types of PCF [36].

When the hole to hole (ʌ) distance are large and diameter of the air-holes are small, it is for high power delivery because a large modal area is obtained, and when the air holes diameter are large and solid core of PCFs is small, a high air filling fraction in the transverse section, so that it is useful for nonlinear allocation like super continuum generation. The structure of periodic arrangement of air holes around the core of the photonic crystal fiber cause the refractive index of the fiber to be changed and effect in the optical properties of the photonic crystal, the air holes of PCFs can be distilled water, liquid crystal, and gas infiltrated, the air holes make the gladding region of the photonic crystal fibers to be tuned by filling

it with liquids that have different refractive index and makes center wavelength of the photonic crystal fibers to be tuned in very wide range[29].

2.3 Guidance Mechanism

In the conventional optical fiber, the light propagation depend on the slight different of the refractive index between two connection regions with different doping levels of the two connection regions for different doping levels of two regions of fiber core and cladding [37].

Actually, photonic crystal fiber guided light by modified total internal reflection mechanism (m-TIR) or the photonic bandgap (PBG) mechanism based on whether the effecting refractive index of the cladding is lower or higher than the refractive index of the core [38].

On infiltrated liquid crystal material in holey cladding region of the photonic liquid crystal with effective refractive index higher than the silica core of photonic crystal fiber. The guiding properties of the photonic crystal fiber are firstly governed by the antiresonant reflection from multiple cladding region and the transmission spectrum of the structure is resolve by the different of refractive index of the cladding region [39].

When infiltrated the nematic liquid crystal in the cladding region of photonic liquid crystal is subjected to the physical parameter such as temperature, electric field, pressure... etc., the nematic liquid crystal molecules undergo reorientation which leading to change the effective refractive index of the cladding and admit for tuning of photonic band gap transmission. Liquid crystal materials make photonic liquid crystal susceptible to external fields variations, this property can be used to fabricate all-fiber sensors for parameters such as magnetic field, temperature and electric field [20]. According to this fact, the guidance mechanism is divided into the following two types:

2.3.1 Modified Total Internal Reflection

In standard step index optical fiber there is a positive core-cladding refractive index difference, in which the refractive index of the core (n_{core}) is greater than that of the cladding ($n_{cladding}$). Similar case is found in solid core of photonic crystal fiber, i.e. $n_{core}>n_{cladding}$. The guidance mechanism of the light is also similar, in solid core photonic crystal fiber is guided with modified total internal reflection. Figure (2.2) shows the comparison between photonic crystal fiber and step-index fiber. Due to the array holes in the cladding of photonic crystal fiber, there is a bigger index contrast between core and cladding [38].

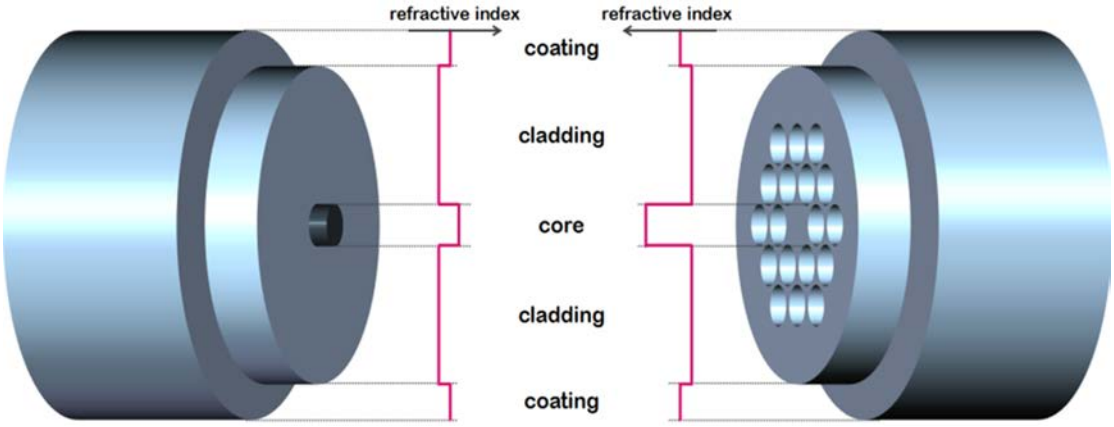

(b) step-index fiber (a) solid-core PCF

Fig (2.2) Geometry and refractive index profiles [38].

Like conventional fiber, if the refractive index of core rather than refractive index of the cladding in the solid core PCF, then the light guided by total internal reflection. Such that, in most all-solid fibers the required index difference is created by doping either core or cladding[37].

2.3.2 Photonic Bandgap Guidance

In silica-air hollow core photonic bandgap fibers light propagate is achieved by several hundreds of holes in triangular lattice arranged around core along the fiber [40]. Total internal reflection are not working in hollow core, so the photonic bandgap is usually met in hollow core PCF ,that accrue when the refractive index in the core is lower than the refractive index in the cladding. Figure (2.3-a) shows

the hollow core PCF cross-section that guided by photonic bandgap and the refractive index profile cross the fiber diameter, whereas Figure (2.3-b) shows the solid core PCF cross section that guided by modified total internal reflection, and the refractive index profile cross the fiber diameter [41].

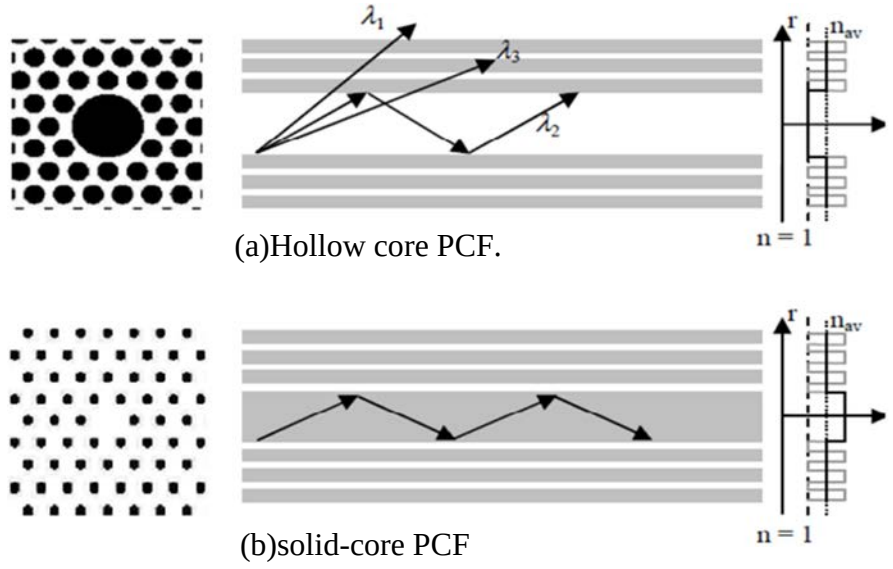

(a)Hollow core PCF.

(b)solid-core PCF

Fig (2.3) Types of photonic crystal fibers [41].

2.4 Loss Mechanisms

There are two types of losses are usually found in photonic crystal fibers; the first type is related to absorption, while the second is related to scattering [42]. The totality of these effects is also known as attenuation. Attenuation varies with the operating wavelength and the type of the fiber as shown in Figure (2.4). The minimum loss in fused silica is noticed at a wavelength of about 1550*nm*, which is lightly less than 0.2 *db/km* [43].

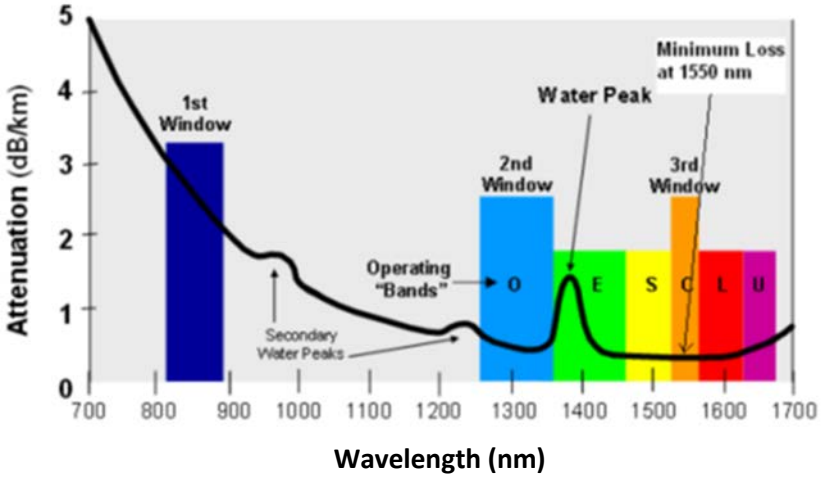

Fig (2.4) Attenuation spectrum of optical fiber [44].

The expression for attenuation α in *dB/km* is given by:

$$\alpha = -\frac{10}{L}\log_{10}\frac{P_0}{P_i} \qquad (1.1)$$

Where, Pi is the input power, Po is the output power, and L is the length of transmission distance measured by (*km*).

Many type of losses in photonic crystal fibers (PCFs) such as scattering absorption, bend loss, and confinement loss. Photonic crystal fibers have very low losses compared with other type of fibers that are used in telecommunications system [45]. More details about types of losses is explained in the following subsections:

2.4.1 Absorption Loss

Absorption loss is the type of attenuation caused by the absorption of photons within fiber at particular wavelengths, which is converted to heat dissipation within the fiber. Absorption losses are intrinsic and extrinsic material properties. Intrinsic absorption occurs by interaction with one or more of the components of the glass. Extrinsic absorption is caused by adding impurities within the glass such as iron chromium to the fiber during the fabrication process [46].

2.4.2 Confinement Loss

In solid-core and hollow-core photonic crystal fibers confinement loss originates by infinite number of air-holes which can be made in the fiber [7]. Low confinement loss is found when the number of the rings of air holes are at least 6 rings and the core of the photonic crystal fibers is small [47]. To reduce the confinement loss, the number of the air holes rings must increase and be careful of the selection of air holes and spacing between adjacent air holes [48]. The confinement (*CL*) can be calculated by means the attenuation constant (*αm*) as follows: [7].

$$CL = 20\log(e) * \alpha m \quad (1.2)$$

$$CL = 8.886 * \alpha m \ (dB/m) \quad (1.3)$$

2.4.3 Bending Loss

The bending losses are categorized into microbend losses and macrobend losses. The microbend losses occur for small-scale bends. It is possible to get a result to waveguide coating, packaging, installation and cabling, and can be decreased through careful processing and handling as show in Figure (2.5), where the mode propagating in the z-direction around a bend of radius R_o in the x-direction. The bending loss in conventional fibers depends on wavelength and only occurs when the long wavelength unlike the bending loss in photonic crystal fibers depend on the bend radius and wavelength [49].

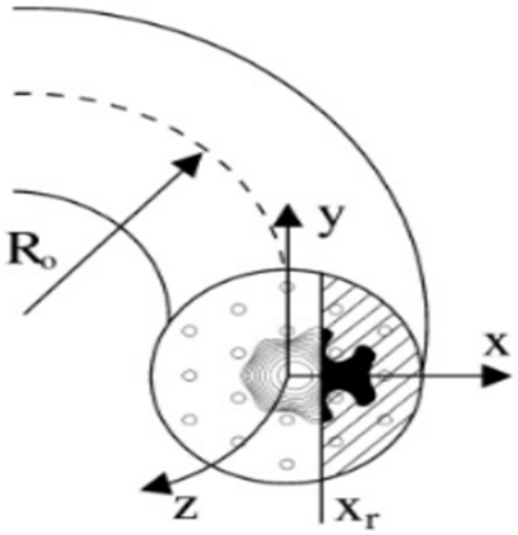

Fig (2.5) Bending loss of PCF [49].

The microbend loss can be expressed as [50]:

$$\alpha_{mic} = 0.05\alpha_m(K^4 * W^6 * \frac{NA^4}{r^2}) \quad (1.4)$$

While the macrobend loss can be expressed as:

$$\alpha_{mac} = -10\log\left(1 - \left\{\frac{1}{2\Delta}\left[\frac{2r}{R} + \left(\frac{3}{2nkR}\right)^{\frac{2}{3}}\right]\right\}\right) \qquad (1.5)$$

Where, Δ is the difference between the core and cladding refractive indices, r is the core radius, R is the radius of the curvature of the bends with proportional to the ratio $(\frac{\Delta^3}{\lambda^2})$, K is the wavevector, NA: numerical aperture, and W is the mode field radius.

2.5 PCF Sensors

Photonic crystal fiber offers a high degree of freedom in design flexibility, facilitating the development of new sensing application by varying in the size and location of the cladding holes and/or the core of the fiber transmission spectrum, dispersion, mode shape, air filling fraction, nonlinearity and birefringence that can be tuned to reach values are not achievable with conventional optical fibers. Moreover, the existence of air holes gives the possibility of the light propagation in air, and provides the ability to infiltration the liquids or gases into the air holes. This enables a well-controlled interaction between light and sample leading to new sensing application. The applications of the photonic crystal fiber in sensing field can be divided into main categories: biosensors, chemical sensor and physical sensor, depending on the parameter that is measured [36].

Physical optic sensors depend on photonic crystal fibers measure physical parameter such as curvature, temperature, displacement, electric field, magnetic field, refractive index, torsion and vibration. The measurement, monitoring, and control of these parameters are of the vast interest for several applications. Physical sensors that assess strain, curvature, torsion, transversal load and temperature are of large interest for structural health monitoring. Civil structures like bridges, buildings, dams need continuous monitoring with the purpose of controlling and preventing abnormal states or accident at an early stage [51]. Other physical sensors like electric field and magnetic field are of enormous benefit for

sensing at high voltages, since they provide an insulating link to high voltage areas not offered by conventional electric sensors [52].

2.5.1 Electric field sensor

In conventional sensors commonly use the antennas, metal connection, or conductive electrodes. In optic sensors widely used in these applications because the fiber optic depend on sensing techniques minimally disarrange the electric field, and part from the sensor head, the connecting fibers are inherently immune to electromagnetic interference.

Unattainable fiber based field sensor should present some properties such as simple design, small size and all fiber configuration with high measurement accuracy [36].

2.5.2 Temperature sensor

Fiber optic in sensor field have proven to be very important in measuring temperature in original metal and glass productions, in power generation operations, oven and automated welding equipment. Another application were in optical fiber depend on the temperature measurement is efficient in high temperature processing operations in cement and chemical industries. This type of fiber optic sensor is the one of the most required in commercial market through the high number of applications in different fields. Accordingly, the temperature sensor based on photonic crystal fibers were quickly developed in order to produce new sensor with improve properties such as sensibility and stability [36].

2.6 Photonic Sensor Setup

Photonic crystal fibers can be used as sensors to measure electric field, temperature, or any other physical quantities by modifying a fiber so that the

property to measure modulates the intensity, phase, polarization, wavelength, or transit time of light in the fiber. Sensors that vary the intensity of light are the simplest, since only a simple source and detector are required. A particularly useful feature of such photonic sensors is that they can provide distributed sensing over distances of up to one meter. Figure (2.6) shows the photonic sensor setup and its basic components.

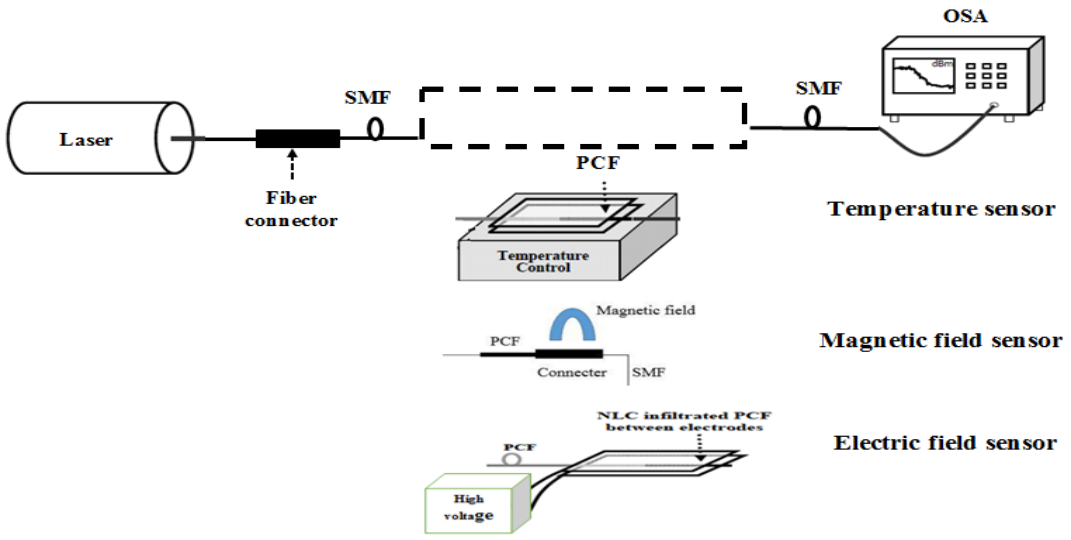

Fig (2.6) Sensor setup of PCF [20].

The temperature effect on the density of EBBA that directly proportional to the refractive index, when the temperature raises lead to a decrease in the density of liquid crystal where due to high temperature the objects is stretch and loss the strength of attraction between molecules and thus get bigger distances between particles and increases the internal molecular movement

The electric field intensity at a point is defined as the force experienced per unit positive charge at a point placed in the electric field, which the electrostatic force per unit charge constituting a field exerting at an arbitrary point, which can be expressed as follows:

$$E = \frac{V}{D} \qquad (1.6)$$

Where, E is the electric field, V is the voltage, and D is the distance between two electrodes plates. For alternating power, the root mean square of the voltage (V_{rms})

is computed by means the maximum value of the voltage (V_{peak}) as given in eq. (1.7), whereas the intensity of the electric field is computed by using V_{rms} and d as follows [20]:

$$V_{rms} = \left({}^{3}/_{8}\right)^{\frac{1}{2}} V_{peak} \qquad (1.7)$$

$$E\_field\ intensity = {}^{V_{rms}}/_{d} \qquad (1.8)$$

2.7 Transmission Intensity

Transmittance of the surface of a material is its effectiveness in transmitting radiant energy. It is the fraction of incident electromagnetic power that is transmitted through a sample, in contrast to the transmission coefficient, which is the ratio of the transmitted to incident electric field.

The decibel-milliwatts (dBm, or dB_{mW}) is referring to the power ratio in decibels (dB) of the measured power referenced to one milliwatt (mW). It is used in radio, microwave and fiber optic networks as a convenient measure of absolute power because of its capability to express both very large and very small values in a short form. Compare dBW, which is referenced to one watt (1000 mW). Since it is referenced to the Watt, it is an absolute unit, used when measuring absolute power.

A power level of 0 dBm corresponds to a power of 1 mW. And 3dB increase in level is approximately equivalent to doubling the power, implies, a level of 3dBm corresponds roughly to a power of 2mW. For each 3dB decrease in level, the power is reduced by about one half, making $-3dBm$ correspond to a power of about 0.5mW. To express an arbitrary power P in milliwatt as x in dBm, or vice versa, the following equivalent expressions may be used [53]:

$$x = 10 \log_{10} \frac{P}{1\mathrm{mW}} \tag{1.9}$$

Idem with *P* in watts

$$x = 30 + 10 \log_{10} \frac{P}{1\mathrm{W}} \tag{1.10}$$

$$P = 1\mathrm{mW} \cdot 10^{\frac{x}{10}}$$

$$P = 1\mathrm{W} \cdot 10^{\frac{x-30}{10}} \tag{1.11}$$

Where *P* is the power measured in Watt and *x* is the power level measured in decibel-milliwatts.

CHAPTER THREE

PROPOSED PCF SENSOR DESIGN

CHAPTER THREE

PROPOSED PCF SENSOR DESIGN

3.1 Introduction

Sensor design is an important part of the photonic fibers field. Extrinsic fiber optic sensors use an optical fiber cable to transmit modulated light from an electronic sensor connected to an optical transmitter. A major benefit of extrinsic sensors is their ability to reach otherwise inaccessible places. An example is the measurement of temperature inside aircraft jet engines by using a fiber to transmit radiation into a radiation pyrometer outside the engine. Extrinsic sensors can be used in the same way to measure the internal temperature of electrical transformers, where the extreme electromagnetic fields present make other measurement techniques impossible.

The design of the photonic fiber sensor is still challenge due to each design is performed for specific application for reaching the optimal efficiency of sensing. It is not possible to state which sensor design is best for all application as the characteristic of each case and the circumstances for each study vary so greatly. Therefore, it is essential to understand the alternative strategies for the sensing so that the most appropriate sensor is selected for the case in hand. At present, there are different sensing procedures used for different purposes by various researchers, each needs some requirements and gives limited results. The search on the best appropriate one still exists to view.

This chapter is concerned with the employed methods of the proposed temperature and electric field sensor design; these methods will be explained and discussed in details for each stage in the workflow, including the liquid crystal preparing stage.

3.2 Proposed PCF Sensor Design

The concept of multi-stage of preparing and designing has been used to establish the proposed PCF sensor. It is claimed that these stages can beneficially be combined and that, through the combination, a significant simple and efficient PCF sensor can be achieved.

The generic structure of the proposed design is shown in Figure (3.1). It is shown that the proposed method is designed to be consisted of two phases: the preparing and design. The preparing is a primary stage, it is responsible on preparing the liquid crystal using its chemical components to be injected in the photonic fiber. Whereas the design is a setup stage, which is responsible on construct the sensor components to be used in the next testing stages. The test stages include examining the sensitivity of the proposed sensor in terms varying the temperature and electric field. The employed measure is the power intensity as a function of temperature once and electric field another time, the measurements of power intensity requires to fixing some related parameters such as wavelength and temperature. More details about each stage are given in the following sections:

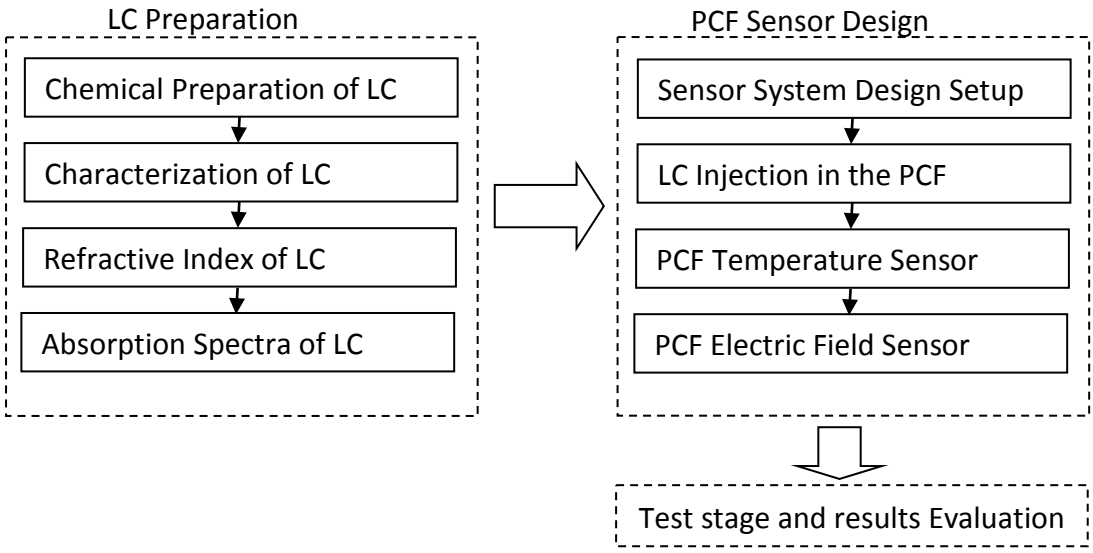

Fig (3.1) Work flow of the proposed PCF sensor design.

3.3 LC Preparation

The nature of a crystallization process is governed by both thermodynamic and kinetic factors, which can make it highly variable and difficult to control. Factors such as impurity level, mixing regime, vessel design, and cooling profile can have a major impact on the size, number, and shape of crystals produced. The preparation phase concerned with preparing the liquid crystal using some chemical components, and then determining its physical characterization of the produced liquid crystal to ensure its correct construction and purity. The following subsections illustrate the preparation and examination stages of the produced liquid crystal with details:

3.3.1 Chemical Preparation of LC

The first stage in the present work is the preparation of the liquid crystal from its chemical components. The adopted liquid crystal is of type N-(4`-ethoxybenzylidene)-4-n-butylaniline (EBBA), which requires to use the chemical materials listed in Table (3.1). The preparation process needs to pass through the following two steps:

Table (3.1): Chemicals and their manufacturers.

Compound	Supplied from
4-hydroxybenzaldehyde	Merck
anhydrous k2co3	BDH
Cyclohexane	Merck
ethyl bromide	BDH
4-n-bytylaniline	BHD
Ethanol (Absolute)	BHD
glacial acetic acid	BHD

Step1: Preparation of N-4'-ethoxybenzylidene: A mixture of (1.1g) 4-hydroxybenzaldehyde and (2.76g) of anhydrous k_2co_3 were dissolved in (4ml)

cyclohexanone, (0.008mol) of appropriate ethyl bromide was added, and the mixture was refluxed with vigorous stirring for overnight as shown in Figure (3.2). The mixture was filtered, the solvent was distilled off. The mechanism of the synthesis of N-4'-ethoxybenzylidene was shown in the Figure (3.3).

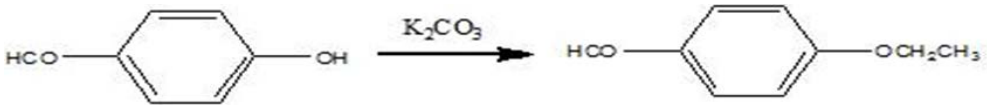

Fig (3.2) Reaction equation to the prepared N-4'-ethoxybenzylidene.

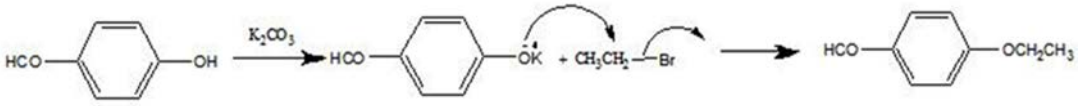

Fig (3.3) Mechanism to the formation of N-(4`-ethoxybenzylidene).

Step2: N-(4'-ethoxybenzylidene)-4-n-butylaniline (EBBA) was prepared from the condensation reaction of N-4-ethoxybenzaldehyde(1.5mL) and 4-n-butylaniline(1.6mL) in absolute ethanol (20mL)with two drops glacial acetic acid was refluxed with stirring for four hours. The formed precipitation was filtrated and recrystallized from ethanol to give N-(4'ethoxybenzylidene)-4-n-butylaniline according to the reaction shown in Figure (3.4). The mechanism of the synthesis of EBBA was shown in the following Figure (3.5).

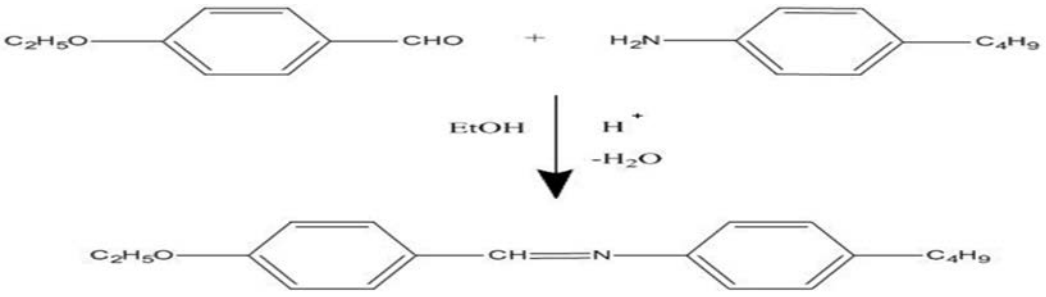

Fig (3.4) Reaction equation to the prepared EBBA.

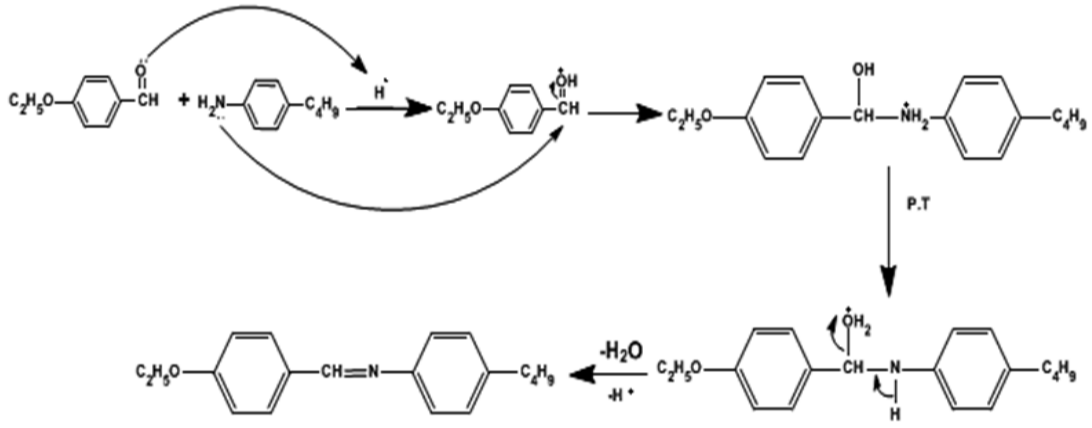

Fig (3.5) Reaction mechanism to the formation of N-(4`-ethoxybenzyli -dene)-4-n-butylaniline.

3.3.2 Characterization of Liquid Crystal

This stage is decided to be carried out for credit correct behavior of physical characteristics of the liquid crystal that made in the laboratory. The considered physical characterization is the transmittance of the adopted liquid crystal, the behavior of the transmittance is considered as a function to the different wavelengths.

3.3.3 Fourier Transform Infrared Spectroscopy (FTIR)

Fourier Transform Infrared Spectroscopy (FTIR), which is used to record the spectrum of potassium bromide disk on IR-presige21 model, Shimazu, 2006, Iraq, Baghdad, university of Baghdad.this device is used to record the spectrum of EBBA liquid crystal for notes the change of function grope of material.

3.3.4 Refractive Index of LC

Abbe refractometer with wavelength (ƛ=589.3 nm) and the accuracy equal to ±0.001 nD using a HAKKE-D1-G thermometer water bath and a Hewlett-Packard model 201Aquartz thermometer can be used to measure the refractive indices of prepared compound of EBBA liquid crystal material with different temperature. The acceptable values of such indices are indicating light paths inside the PFC.

3.3.5 Absorption Spectra of LC

The UV-Visible spectrophotometer device (UV-160Amodel, Shimadz, Iraq, Baghdad, university of Baghdad) is used to get the absorption spectra of the LC at the region of interest in the wavelength range. The behavior of absorption spectra indicates the useful region of the wavelength that showed maximum amount of absorption. This region can be employed to credit higher efficiency for sensor performance.

3.4 PCF Sensor Design

The PCF sensors of temperature and electric field have been designed by using solid core photonic crystal fiber (LMA-10) for temperature sensor and hollow core photonic crystal fiber (HC-1550) for electric field sensor. The photonic crystal fiber infiltration by capillary effect will be used to sense temperature and electric field. Also, different wavelength in the temperature sensor are decided to be used, whereas there is just one wavelength will be used to test the electric field sensor.

To introduce the designing phase, the designing requirements should first be determined. The following subsections explain these requirements and the next stages that related to the design setup:

3.4.1 Sensor Design Requirements

The setup of the proposed design needs to perform the following processing on the prepared liquid crystal and photonic fiber, this to ensure the efficient performance for the proposed design:

The requirements are the instruments and equipments that needed to establish the PCF sensor design, which are listed as follows:

1. Solid core photonic crystal fiber-(LMA-10), which is a type of photonic crystal fibers produced by NKT Company. This fiber contain of two layer, core and cladding made of from pure silica with diameter equal to (10.1 ± 0.5 µm) and (125 ± 2 µm) respectively and coating this two layer by Acrylate

material with diameter equal to (245 ± 10 μm). This type of PCF will be employed to design the proposed temperature sensor.

2. Hollow core photonic crystal fiber (HC-1550), which is a type of photonic crystal fibers produced by Thorlab Company. This fiber contain of two layer, core and cladding made from silica with diameter ($10\pm1\mu m$) and ($120\mu m$) respectively. This type of PCF will be employed to design the proposed electrical field sensor.

3.4.2 PCF Establishment

The establishment of the PCF requires to join two pieces belong to different types of PCF. This is can be carried out using special technique related to the cleaving and splicing processes. More details about such processes are mentioned in the following:

A. PCF Cleaving

Cleaving process aims to remove coating of the head of the fiber by stripping tools such as the CFs-1 or Fitel S-210. If removal of coating debris was needed, one can use a folded sheet of lint free lens tissue to avoid leakage of liquid into holes. It should be note that the use of any solvent for cleaving the fiber after cleaving process is not allowed since it may cause a failure of connecting and sensing.

B. PCF Splicing

Photonic crystal fiber spices are different from standard fiber splices because the core cannot be seen through the side of the fiber and the power will be reduced, typical splicer power is about 25% less than that used for comparable solid fibers [54], to collapse of the holes. The most challenging problem in splicing PCF, is a voiding the collapse of the microstructures holes, because high temperatures from splice also giving a chance to glass to flow.

There are many splicing techniques used to splice photonic crystal fiber with different fibers, one techniques has been used namely fusion splicers. FSM-

60 splicer that produced by Fujikura Company has been used to splice different types of fiber, LMA-10 PCF spliced with a single mode fiber (SMF-28) from one end. The other end of PCF LMA-10 was connected by a free space connector to give an access for liquid infiltration.

The present setup comprises of a piece of LMA-10 photonic crystal fiber spliced from one end with single mode fiber SMF-28. The other end of the LMA-10 photonic crystal fiber was connected to give an access for liquid infiltration by free space connector. Figure (3.6) show the splicing of photonic crystal fiber with single mode fiber.

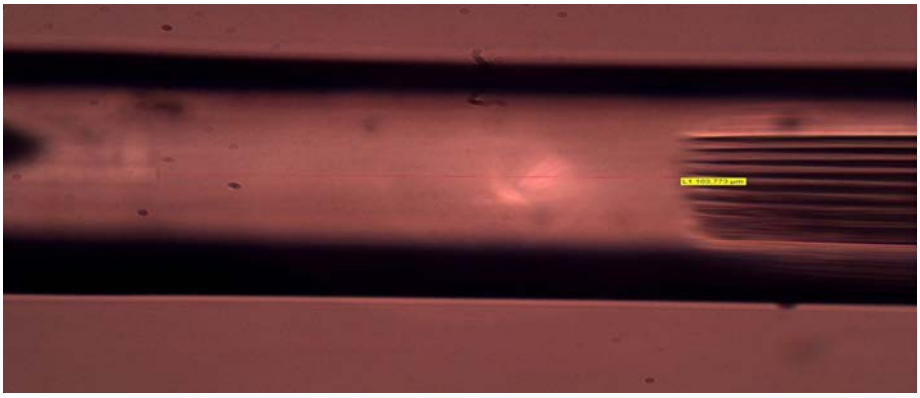

Fig (3.6) PCF-SMF splicing.

3.4.3 LC Injection in PCF

The injection of LC in the PCF in this work by using capillary tube method, this method is used because the techniques of injection is unavailable. By this method can LC a rise in PCF approach *1cm.*

3.5 PCF Infiltration Temperature Sensor

This type of sensor based on use a small piece of EBBA infiltrated with fluid sensitive to temperature. Where, EBBA was infiltrated through the photonic crystal fiber by means of capillary effect, time article to be taken to rise almost an hour. This fluid is used with solid core LMA-10 PCF at different temperature and different wavelengths (1550, 1060, 850 *nm*) and laser helium-neon with 632.8 *nm*.

Such that, photonic crystal fiber will become sensitive to temperature, and this will have effects the output light power through the filled photonic crystal fiber.

the experimental setup of the temperature sensor is shown in Figure (3.7), whereas Figure (3.8) shows the photograph of photonic crystal fiber infiltrated with prepared liquid crystal.

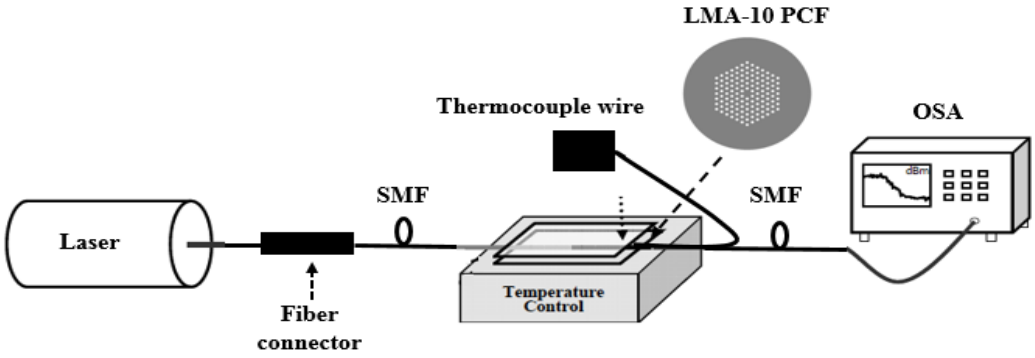

Fig (3.7) Setup of the temperature sensor photonic crystal fiber.

Fig (3.8) Infiltrated with prepared liquid crystal.

The diode laser shown in Figure (3.9) is used to provide laser beams of different wavelengths 1550, 1060, 850 *nm*, the power of such laser almost 1*mw*. Also, the helium-neon laser is used to provide a laser beam of wavelength 632.8 *nm*.

The fiber of type LMA-10 PCF is used as a sensor head, such type consist of a six rings of air holes surrounded the solid core as mentioned in appendix. The optical spectrum analyzer OSA(YOKOKKAWA, Ando AQ6370) with resolution 0.02 *nm* was used to monitor the interference spectra of the sensor. Also a hot plate (Thermostiertific type 1900) is used in addition to thermo couple wire of type K.

Full collapsing technique was used to connect photonic crystal fiber to single mode fiber. Before splicing PCF with SMF, they are cleaved by high precision cleaver (CT-30), then they are spliced by fusion splicing machine (FSM-60). A free space connector with less loss is used to connect them from other side to give an access for liquid infiltration as shown in Figure (3.10).

Fig (3.9) Photograph of laser diode (1550, 850,1060) nm.

Fig (3.10) Free space connector.

3.6 PCF Infiltration Electric Field Sensor

This type of sensors based on use a small piece of hollow core photonic crystal fiber infiltrated with liquid. Where, the open end of the photonic crystal fiber was infiltrated with EBBA liquid crystal at room temperature by dipping the cleaved and into the liquid crystal material. The liquid crystal material was drawn into the holes of photonic crystal fiber by capillary action and an infiltration length ~1 *cm* was obtained.

The electric field is applied to the infiltrated photonic crystal fiber by means of two electrodes positioned on opposite sides at the infiltrated end of the photonic crystal fiber. The distance between two electrodes is equal to the 0.25 *cm* .The values of voltage in our experiment from zero volt to V_{peak} , the used maximum value of V_{peak} is 700 *V*. the transmission spectra of the infiltrated photonic crystal fiber sample was record by using spectrometer. Figure (3.11-a) shows the photograph of empty hollow core PCF, whereas Figure (3.11-b) infiltrated PCF

with prepared liquid crystal (EBBA). Figure (3.12) shows the fabrication of the electric field sensor setup.

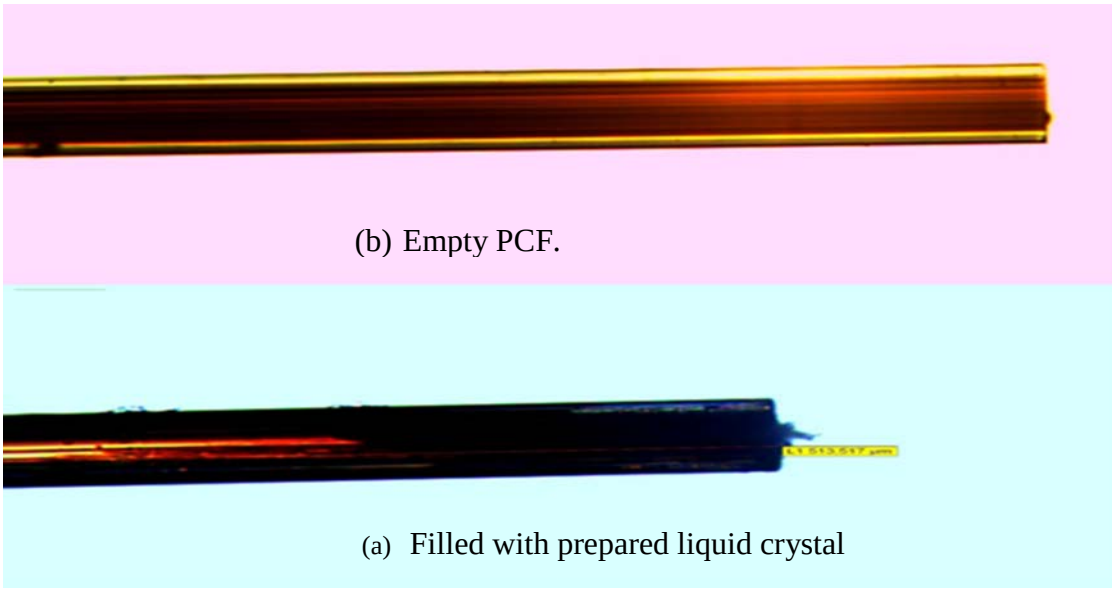

(b) Empty PCF.

(a) Filled with prepared liquid crystal

Fig (3.11): photograph of photonic crystal fiber.

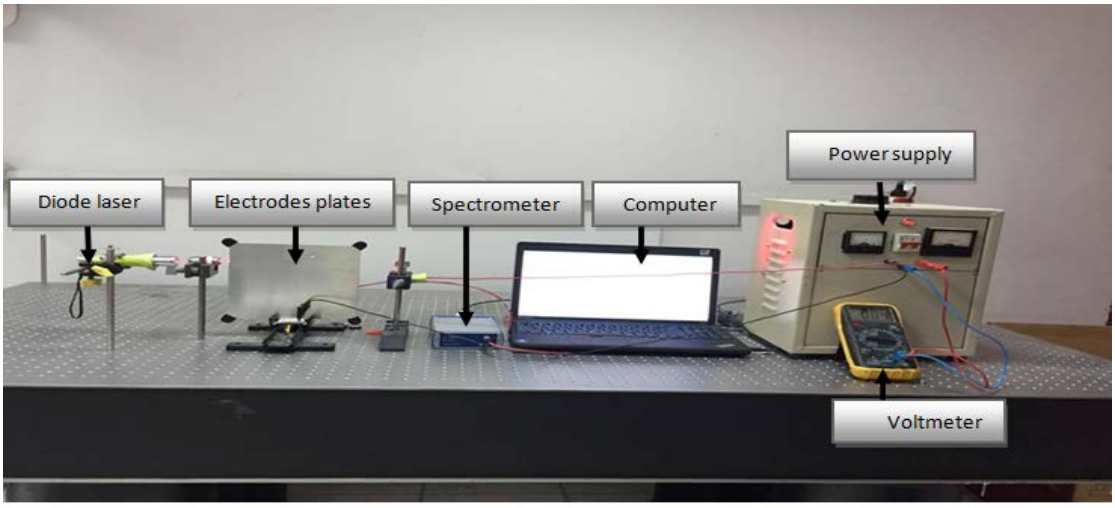

Fig (3.12) Photograph of the setup of the electric field sensor.

The diode laser (produced by ASTRO company) is used with wavelength equal to 650 *nm*, the power of this laser<200 *mw*. The type of the used fiber as a sensor head is HC-1550 PCF. This fiber set between two electrodes plates of spacing distance is equal to 0.25 *cm*. The spectrometer (of type; Ava Spec_2048 XL, produced by AVANTES company) was used to record the transmission spectra with increasing the voltage by using high voltage power supply (100-1000 *V*) and voltmeter (of type; 3PK-600T, produced by Proskit company). Also there

is an objective lens is used to focus the light of the laser on the head of fiber as shown in Figure (3.13).

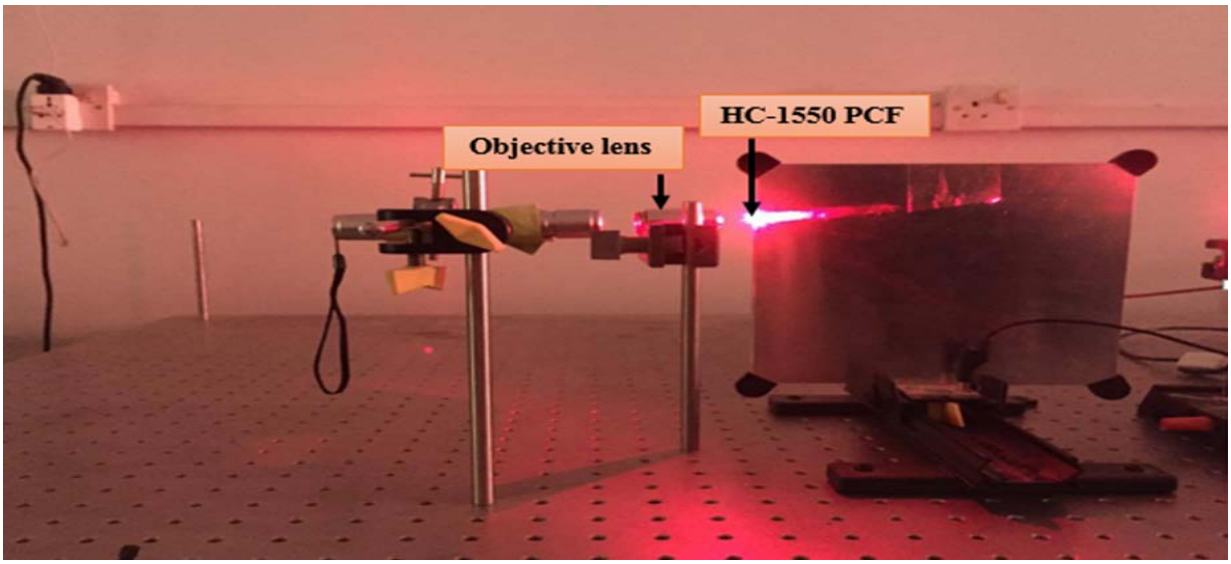

Fig (3.13) Photograph of the setup of the electric field sensor with an objective lens.

3.7 Test Results Evaluation

Last stage is the performance efficiency determination, which is a comparison based on power intensity between the achieved results and that mentioned in the literatures, the result of the comparison will determine the performance efficiency with consideration of setup and material difference from that of literatures, which help to decide the ability exporting the proposed sensor in to application field.

CHAPTER FOUR

RESULTS AND ANALYSIS

CHAPTER FOUR
RESULTS AND ANALYSIS

4.1 Introduction

The development of PCF based liquid crystal brings about an easy way to extract useful techniques in broad applications. Consequently, the data analysis extracted from the behavioral performance of temperature and electric field sensors is examined using validation and assurance techniques. In the present work, there are two considered paths; training and sensor design. The training is the practical way by which the liquid crystal is prepared, and then determining its physical characterization, while the sensor design uses the prepared liquid crystal to produce sensors in terms of temperature and electric field variations. Results analysis is then carried out for validation purpose. The analysis includes a presentation about how implement the methods mentioned in the previous chapter. Also, there is a detailed explanation related to the results achieved through implementing each stage in the proposed PCF sensor design method. The results are presented in figures and tables including quantitative and qualitative analytical discussions. Then, this analysis is estimated to evaluate the performance of the proposed sensors. The following sections show more details about the results and analysis of the employed method.

4.2 LC Preparing Results

The liquid crystal N-(4'ethoxybenzylidene)-4-n-butylaniline (EBBA) was prepared from condensation reaction of N-4-ethoxy benzaldehyde and 4-n-butylaniline according to the reaction show in Figure (3.4). This EBBA possess a transition temperature range between (36n-80i)^{0}C. The liquid crystal molecules depended on the temperature where below $36^{0}C$, where the molecules of such material become solid and become a liquid above $80^{0}C$ as illustrated in Figure (4.1). The following subsections explain the physical measurments applied on the prepared EBBA to ensure its quality assurance.

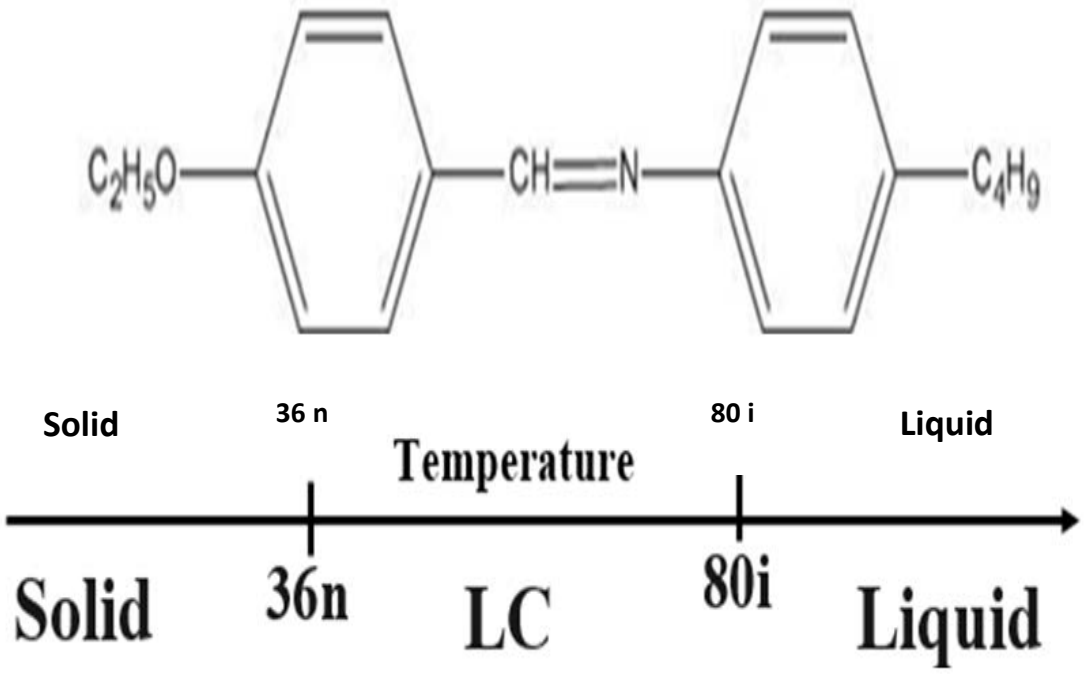

Fig (4.1) Transition temperature range for EBBA liquid crystal.

4.2.1 LC Characterization Results

The prepared compound was identified by FTIR spectroscopy. The characteristic bands of EBBA, 4-n-butylaniline, and 4-ethoxybenzaldehyde are shown in Figures (4.2), (4.3), and (4.4) respectively. Compound of EBBA shows the appearance of band at 3020 cm^{-1} that attributed to the υ (C-H) arome. Groups, bands at. 2954.95, 2927.94, 2858.51 cm^{-1} assigned to the asymmetrical and symmetrical stretching of (C–H) aliphatic, respectively, the imine band appeared at 1616.35 cm^{-1}, bands at 1516.05 cm^{-1}, 1118.71 cm^{-1}, and 829.39 cm^{-1} that are due to υ (C=C), υ (C-O), and out of plane bending of para dis substituted benzene ring respectively. The disappearance of the υ (NH_2) group for amine and υ (C=O) group of aldehyde are also detected.

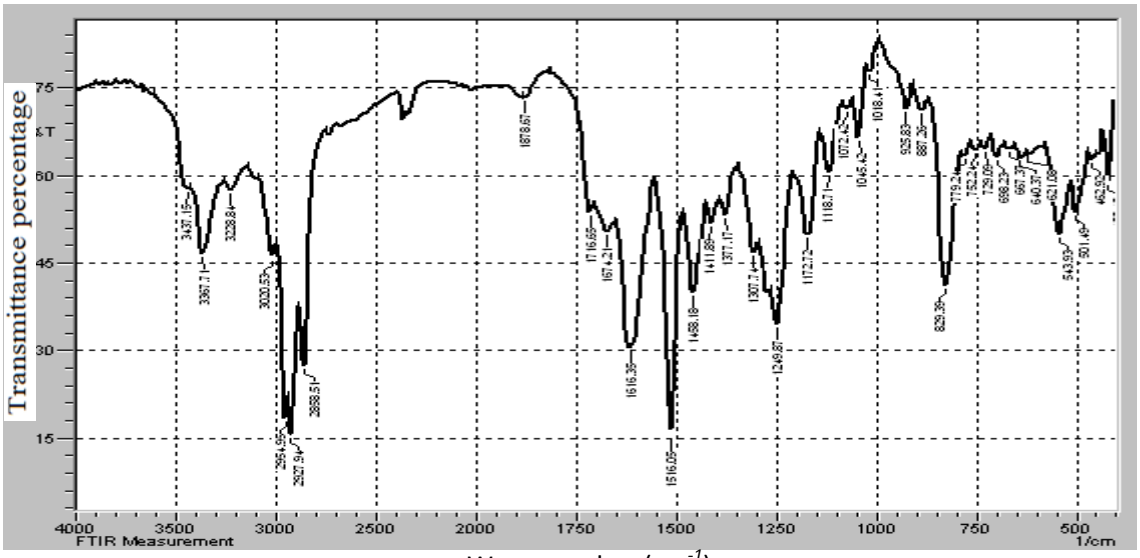

Wave number (cm^{-1})

Fig (4.2) FTIR spectrum of EBBA.

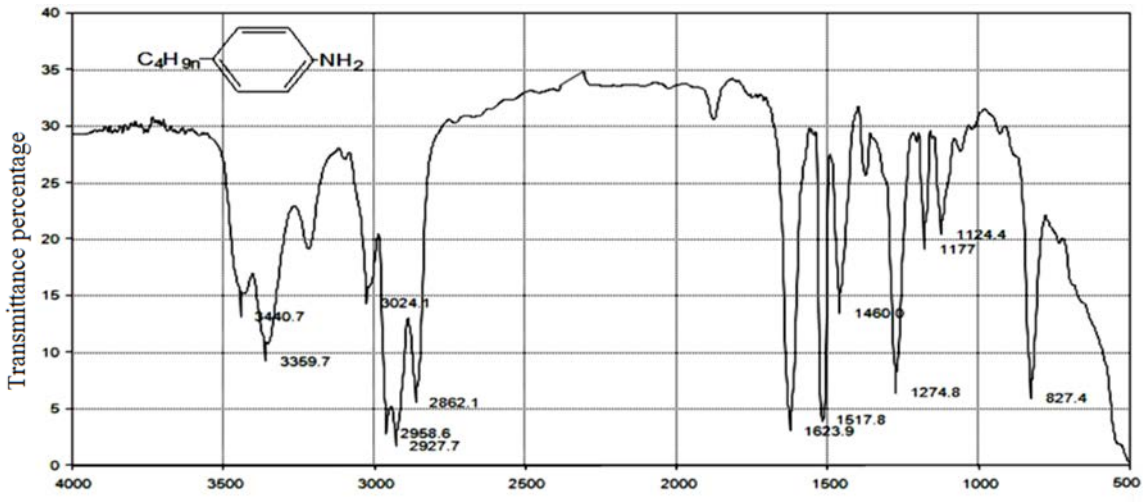

Wave number (cm^{-1})

Fig (4.3) FTIR spectrum of 4-n-butylaniline.

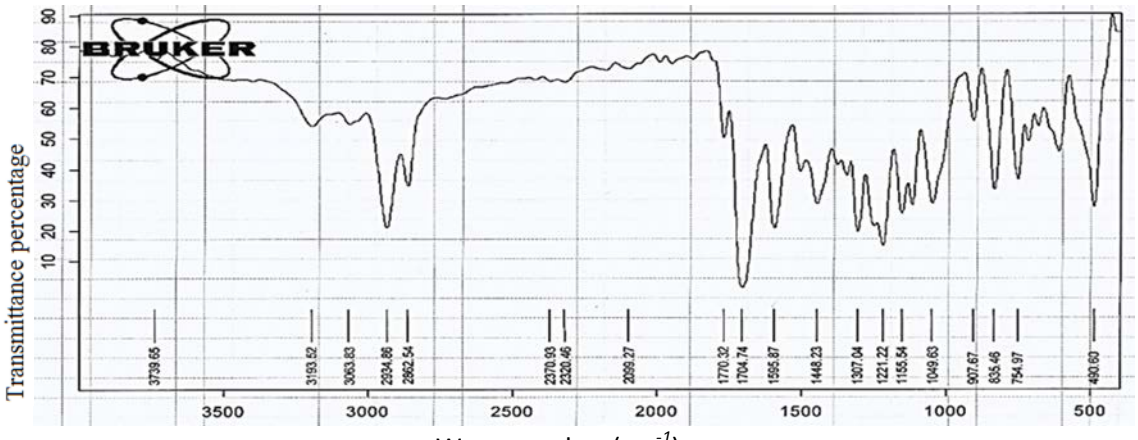

Wave number (cm^{-1})

Fig (4.4) FTIR spectrum of 4'-ethoxybenzylidene.

4.2.2 LC Refractive Index Results

Abbe refractometer is used to measure the refractive index of EBBA many times with varying the temperature of EBBA, measurements were recorded using sodium D line of wavelength λ=589.3*nm* and temperatures range (25-80^{o}C). The result shows that the increase of temperature leads to decrease the index of refraction values of EBBA (1.3284–1.3198) as given in table (4.1).

Throughout the refractive index measurements, the temperature is using a HAKKE-D1-G thermometer water bath and a Hewlett-Packard model 201Aquartz thermometer that work in the visible light region, in which the refratometer was connected to the water bath. Figures (4.5) refer to the relationship between the refractive indices of EBBA and temperature through the heating process.

Table (4.1): The values of refractive index of EBBA with changing temperature.

Temperature(^{o}C)	**$n_{heating}$ ±0.001**
25	1.3284
30	1.3273
35	1.3268
40	1.3250
45	1.3246
50	1.3237
55	1.3234
60	1.3231
65	1.3229
70	1.3200
75	1.3198
80	1.3194

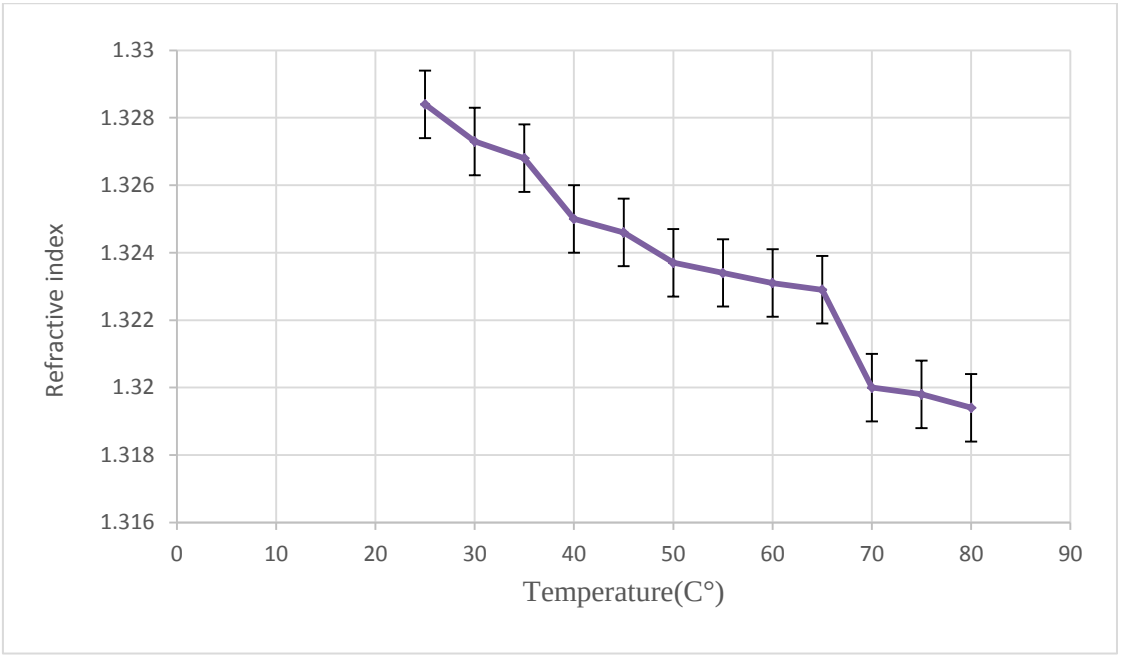

Fig (4.5) Shows the variation of refractive index of EBBA with temperature in the heating process.

It is shown that the refractive index of EBBA shows very small variation with temperature, this variation is normal compared with other liquids such as water given in(Alexey N.Bashkatov,Elina A.Genina,2003)[55], and 4-Methoxy-Benzylidene-4-Butyl-n-Aniline (MBBA) liquid crystal given in(Abdul-Aziz O.M,Abdul-karim J.R et al,2013) [56].

The values of the refractive index are gradually decreasing with increasing the temperature. This is due to the density of EBBA that directly proportional to the refractive index, when the temperature rises lead to a decrease in the density of liquid crystal where due to high temperature the objects is stretch and loss the strength of attraction between molecules and thus get bigger distances between particles and increases the internal molecular movement. Stretch objects leads to the decrease in the density of matter and thus decrease the refractive index.

4.2.3 LC Absorption Spectra Results

Figure (4.6) shows the absorption behavior of the EBBA along the wavelength range (200-900 *nm*). It is shown that the maximum absorption value of the LC at the wavelength (λ_{max}=246 *nm*).

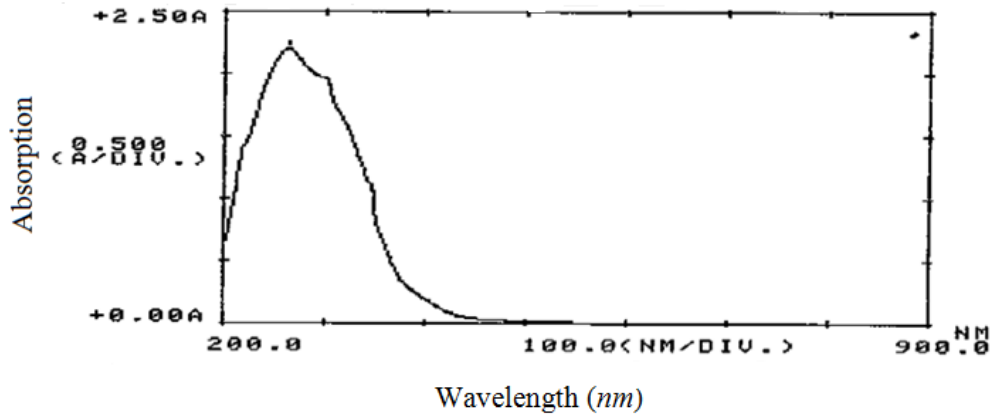

Fig (4.6) the absorption behavior of EBBA measured using UV-Visible.

The behavior of absorption spectra indicates the useful region of the wavelength that showed maximum amount of absorption. This region can be employed to credit higher efficiency for sensor performance for this reason used wavelength large than 246 nm to avoide the absorption of material to light so, can be obtained high output power .

4.3 PCF Temperature Sensor Test

The used PCF in the temperature sensor is composed to two pieces; the first is a solid core LMA-10 PCF that spliced to the second piece of type SMF-28. The characteristics of such types of PCF are presented in appendix.

Different sensor configuration has been constructed with different infiltrated liquids. One type of photonic crystal fibers which is LMA-10 was used to carry experiment applying with different wavelengths (1550, 1060, 850, and 632.8 *nm*).the values of the power change to the value of transmission intensity by using equation (1.9).

Table (4.2) listed the resulted temperature and transmission with the variation of temperature at wavelength (1550 ,1060,850,and 632.8 nm). This refers to that there is a relation between the refractive index distribution over air holes and temperature change of the spectrum with increasing temperature. Figures (4.7-4.10) show the behavior of the transmission with the variation of temperature. It is

found that the sensitivity of the temperature sensor by the slope is (0.02, 0.008971, 0.004536, and 0.002607 $dBm/^{o}C$) respectively.

Table (4.2)the results of photonic crystal fiber temperature sensor infiltrated with EBBA liquid crystal of (1550,1060,850,and 632.8 nm)

Temperature°C	λ= 1500 (nm)		λ= 1060 nm		λ=850 nm		λ=632.8 nm	
	Power(mW)	Transmission (dBm) ± 0.02	Power(mW)	Transmission (dBm) ± 0.02	Power(mW)	Transmission (dBm) ± 0.02	Power(mW)	Transmission (dBm) ± 0.02
20	0.0027542	-25.6	0.0002911	-35.35	0.00930	-20.31	0.00640	-21.93
30	0.002884	-25.4	0.000304	-35.171	0.00934	-20.29	0.00643	-21.91
40	0.00302	-25.2	0.0003111	-35.07	0.00942	-20.25	0.00647	-21.89
50	0.0031622	-25.0	0.0003165	-34.99	0.00952	-20.21	0.00651	-21.86
60	0.0033113	-24.8	0.0003205	-34.94	0.00960	-20.17	0.00654	-21.84
70	0.0034673	-24.6	0.0003269	-34.85	0.00975	-20.10	0.00659	-21.81
80	0.0036307	-24.4	0.0003332	-34.77	0.00990	-20.04	0.00664	-21.77

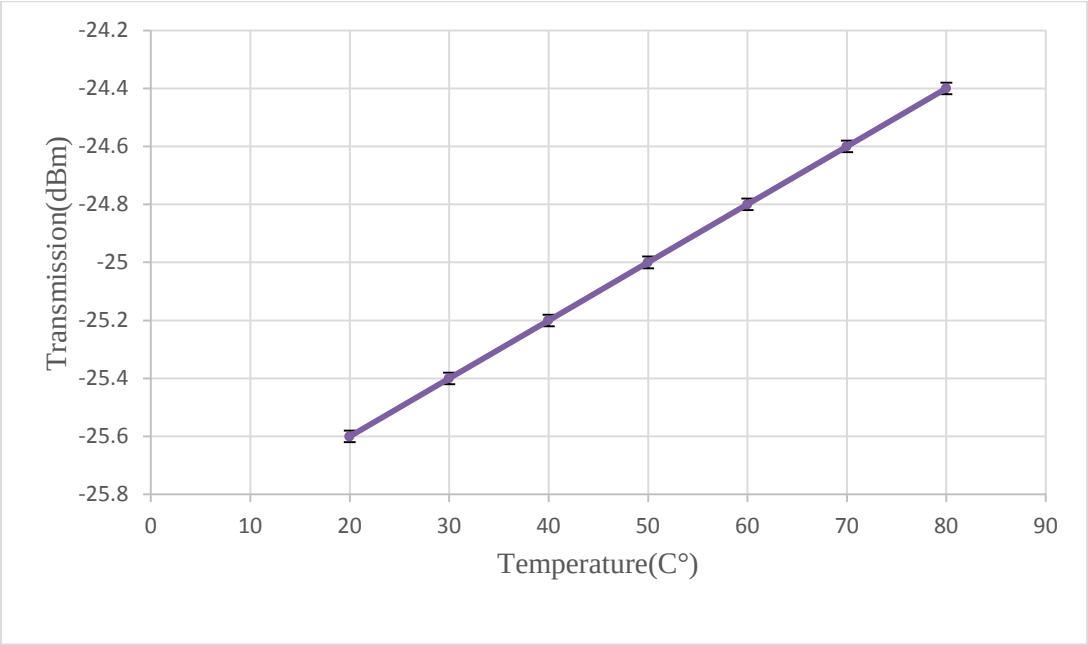

Fig (4.7) The relation between transmission and temperature after infiltration with EBBA liquid crystal at 1550 *nm*.

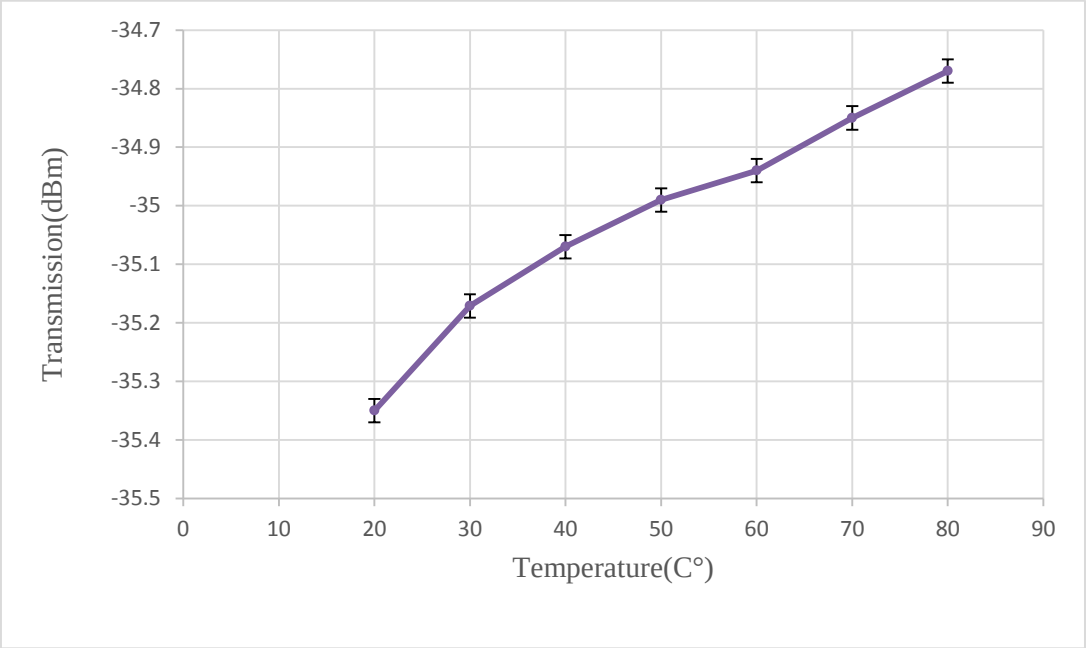

Fig (4.8) The relation between transmission and temperature after infiltration with EBBA liquid crystal at 1060 *nm*.

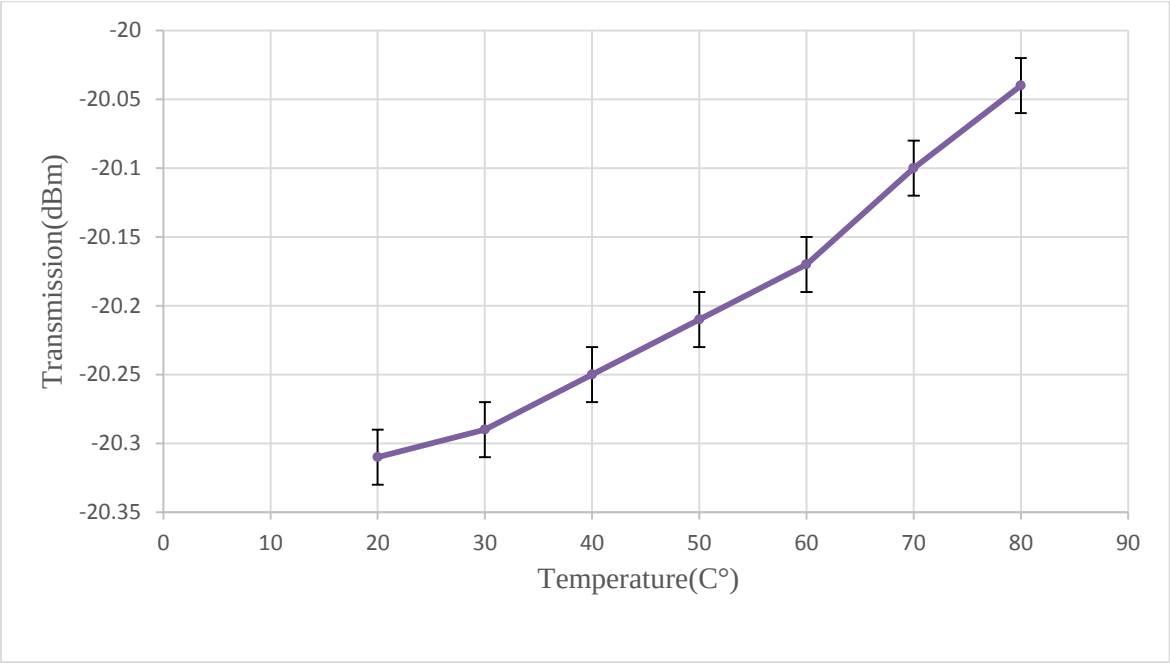

Fig (4.9) The relation between transmission and temperature after infiltration with EBBA liquid crystal at 850 *nm*.

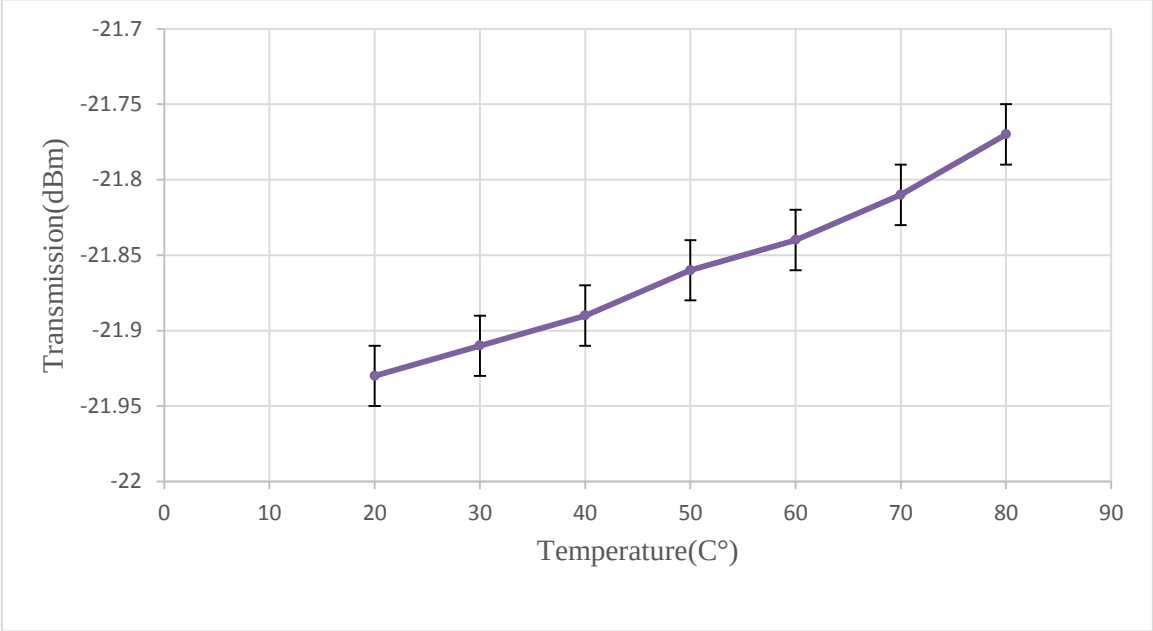

Fig (4.10) The relation between transmission and temperature after infiltration with EBBA liquid crystal at 632.8 *nm*.

The results have shown that the transmission have been increased with increasing the temperature, this is due to influence refractive index on the propagation mode that becomes less confined in the fiber.

Table (4.3) and Figure (4.11) summarize the results of this part of the experiment.

Table (4.3): shown the relation between sensitivity to temperature and wavelength**.**

Wavelength (nm)	**Sensitivity (dBm/°C)**
1550	0.020000
1060	0.008971
850	0.004536
632.8	0.002607

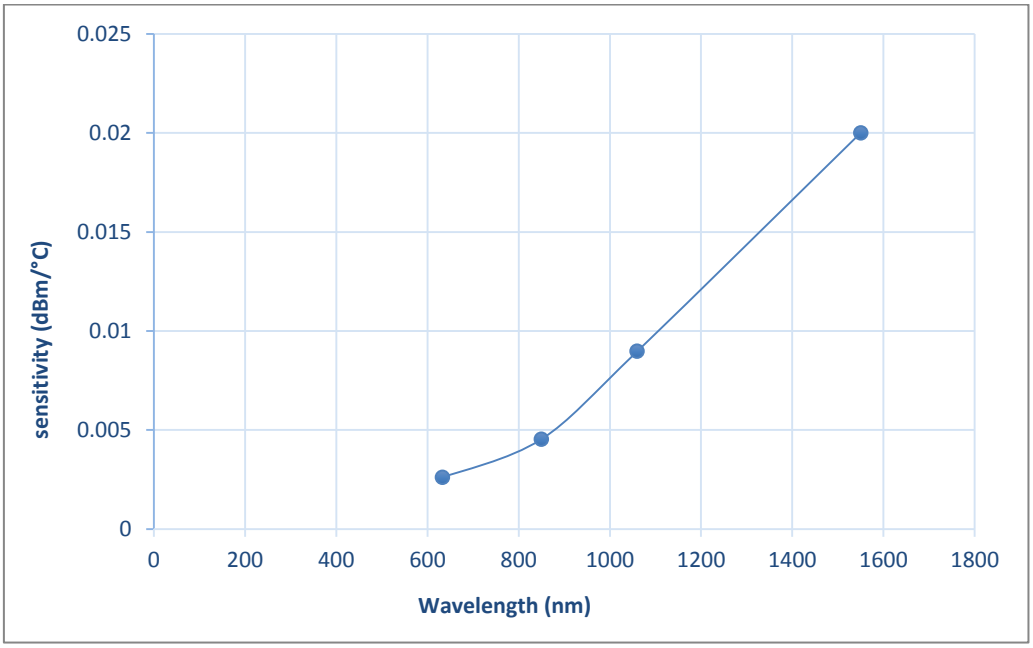

Fig (4.11) Sensitivity of temperature at different wavelength.

From figure (4.11) the result have shown that the increasing in temperature affect on the molecules of liquid crystal and photons emerging from liquid crystal through the fiber. This increase in temperature leads to increased the vibrating

energy of the liquid crystal, because of the strong bonds between the liquid crystal molecules, the effect does not appear that not much vibrating liquid crystal molecules only a very slight vibration of possible neglecting.

In addition, the increased in temperature also leads to increased kinetic energy of the photons, and this makes the largest number of photons is implemented through the liquid crystal down to spectrometer. This means an increase in the power of light emerging from the fiber and thus lead to increase transmission with different wavelengths , but at wavelength equal to 1550 nm found that the temperature sensitivity as high as possible because at this wavelength be less loss and attenuation as possible(K.Nagayama,M.Kakui et al,2002) [43].

4.4 PCF Electric Field Sensor Test

One type of photonic crystal fiber which is HC-1550 was used to carry experimentally applying with wavelength equal to 650 nm. The values of the voltage can be change to the electric field intensity by using equation(1.8).

It is found that there is a relation between the electric field intensity and transmission as show in Table (4.5).

Table (4.4) the values of voltage and power.

Voltage (V)	Power (mW)
0	0.60496
100	0.60509
200	0.60592
300	0.60586
400	0.60318
500	0.60475
600	0.60949
700	0.60630
800	0.60650
900	0.60660

Table (4.5) The values of electric field intensity and transmission.

Electric field intensity (V_{rms}/mm)	**Transmission (*dBm*)**
0	-2.18
24.48	-2.18
48.96	-2.18
73.44	-2.18
97.92	-2.19
122.4	-2.18
146.8	-2.15
171.3	-2.17
195.9	-2.17
220.4	-2.17

The transmission response of the device with increasing electric field intensity is shown in figure (4.12).between a field intensity of zero and 97.92 V_{rms}/mm, the transmission remains unchanged. Above this threshold field intensity, the nematic liquid crystal molecules begin to reorientation which results in a gradual decrease in transmission through the infiltrated photonic crystal fiber with EBBA liquid crystal with the increasing electric field intensity until an of ~(146.8 V_{rms}/mm) is reached.

The transmission response in the electric field intensities from 97.92 V_{rms}/mm to 146.8 V_{rms}/mm is close to linear. The linear part of the transmission response for the infiltrated photonic crystal fiber in the electric field intensity show that the sensitivity to the electric field equal to 0.00123 dBm/(V_{rms}/mm).

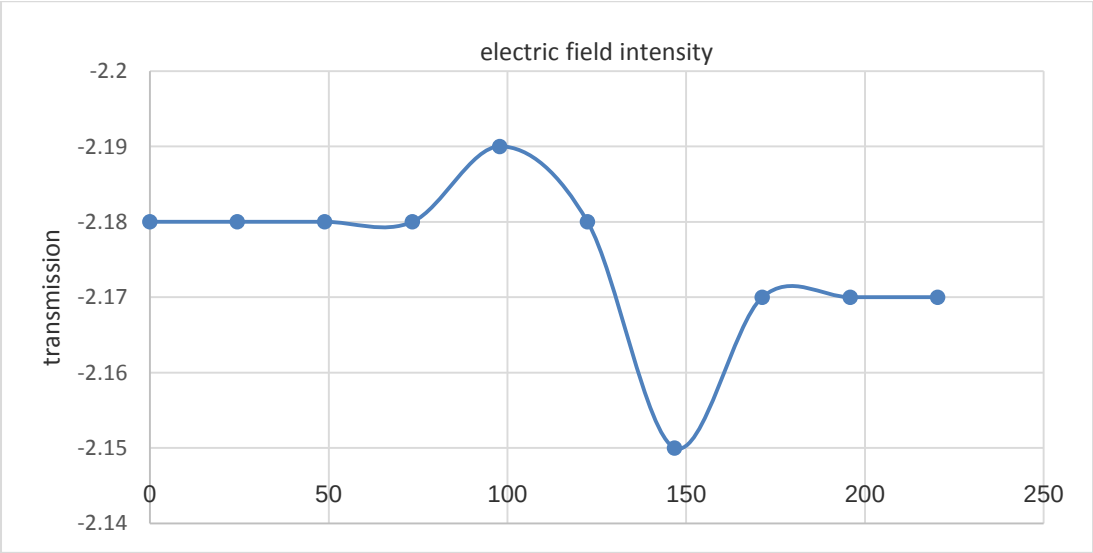

Figure (4.12): shows the relation between transmission and electric field intensity after infiltration with EBBA liquid crystal at 650 nm.

In order to measure the sensor sensitivity, it should be take in a count just the region that the sensor operate through this refers to the interval 97.2-146.8 *Vrms/mm* of electric field intensity, but the last literature mention that the best description of the sensor sensitivity is linearly when the behave of the sensor is decay with increasing transmission intensity, which is the region between 97.2-146.8 *Vrms/mm*.

CHAPTER FIVE

CONCLUSIONS

AND FUTURE WORK

CHAPTER FIVE

CONCLUSIONS AND FUTURE WORK

5.1 Conclusions

Throughout the implementation of the present work, a number of conclusions have been achieved based on the practical results. The following statements summarize the most important ones:

- The values of refractive indices decrease with increasing temperature in thermal range(25-80)℃, so this liquid crystal material(EBBA) have good property for different thermo-optics applications such as temperature sensors.
- The temperature sensitivity of a LMA-10 PCF infiltration with EBBA liquid crystal was measured and it showed:

The sensitivity for temperature sensor infiltrated with EBBA liquid crystal is (0.02, 0.008971, 0.004536, and 0.002679 dBm/ ^{o}C) at wavelength (1550, 1060, 850, and 632.8 nm) respectively.

From this values of sensitivities the highest temperature sensitivity at wavelength equal to 1550 nm, because the minimum loss in fused silica less than 0.2db/km

- The electric field sensitivity of HC-1550 PCF infiltration with EBBA liquid crystal was measured and equal to 0.00123 dBm/ (V_{rms} /*mm*).
- EBBA liquid crystal sensitive to temperature more than sensitive to electric field, because the liquid crystal molecules change phase by increase or decrease temperature.

5.2 Suggestions for Future Work

There are some suggestions taken into account for developing the implementation of the present work, which help to achieve a higher level of performance efficiency, they are given in the following:

1. The EBBA liquid crystal can be used in other type of sensors such as, refractive index sensor, and pressure sensor
2. The use of nanomaterial technology for preparing injected material can be used to produce a magnetic field sensor.
3. The use of COMOSOL program is useful for designing and simulating any sensor, and then compare its results with the experimental ones.

REFERENCES

[1] J. Eichenholz, "Photonic-crystal fibers have many uses," *Optoelectronics World, August,* 2004.

[2] A. Ghatak and K. Thyagarajan, *An introduction to fiber optics*: Cambridge university press, 1998.

[3] L. Bigot and P. Roy, "Fibres à cristal photonique: 10 ans d'existence et un vaste champ d'applications," *Images de la physique,* pp. 71-80, 2007.

[4] S S. A. Cerqueira Jr, "Recent progress and novel applications of photonic crystal fibers," *Reports on progress in physics,* vol. 73, p. 024401, 2010.

[5] J. Knight, T. Birks, P. S. J. Russell, and D. Atkin, "All-silica single-mode optical fiber with photonic crystal cladding," *Optics letters,* vol. 21, pp. 1547-1549, 1996.

[6] J A. Cusano, M. Consales, A. Crescitelli, and A. Ricciardi, *Lab-on-fiber Technology*: Springer, 2015.

[7] F. Poli, A. Cucinotta, and S. Selleri, *Photonic crystal fibers: properties and applications* vol. 102: Springer Science & Business Media, 2007.

[8] R. Buczynski, "Photonic crystal fibers," *Acta Physica Polonica Series A,* vol. 106, pp. 141-168, 2004.

[9] T. Ritari, *Novel sensor and telecommunication applications of photonic crystal fibers*: Helsinki University of Technology, 2006.

[10] J. A. Paquette, "Synthesis and Investigation of the Liquid Crystalline Properties of Polycyclic Aromatic Hydrocarbons," 2012.

[11] J. Prost, *The physics of liquid crystals*: Oxford university press, 1995.

[12] S. Singh and D. A. Dunmur, *Liquid crystals: fundamentals*: World Scientific, 2002.

[13] T. Wolinski, K. Szaniawska, S. Ertman, P. Lesiak, A. Domanski, R. Dabrowski, *et al.,* "Influence of temperature and electrical fields on

propagation properties of photonic liquid-crystal fibres," *Measurement Science and Technology*, vol. 17, p. 985, 2006.

[14] J. Ju, Z. Wang, W. Jin, and S. Demokan, "Temperature sensitivity of a two-mode photonic crystal fiber interferometric sensor," *IEEE photonics technology letters*, vol. 18, pp. 2168-2170, 2006.

[15] O. Frazao, J. Baptista, and J. Santos, "Temperature-independent strain sensor based on a Hi-Bi photonic crystal fiber loop mirror," *IEEE Sensors Journal*, vol. 7, p. 1453, 2007.

[16] T. R. Woliński, A. Czapla, S. Ertman, M. Tefelska, A. W. Domanski, J. Wójcik, *et al.*, "Photonic liquid crystal fibers for sensing applications," *Instrumentation and Measurement, IEEE Transactions on*, vol. 57, pp. 1796-1802, 2008.

[17] L. V. Nguyen, D. Hwang, S. Moon, D. S. Moon, and Y. Chung, "High temperature fiber sensor with high sensitivity based on core diameter mismatch," *Optics express*, vol. 16, pp. 11369-11375, 2008.

[18] Y. Yu, X. Li, X. Hong, Y. Deng, K. Song, Y. Geng, *et al.*, "Some features of the photonic crystal fiber temperature sensor with liquid ethanol filling," *Optics express*, vol. 18, pp. 15383-15388, 2010.

[19] S. Mathews, G. Farrell, and Y. Semenova, "Directional electric field sensitivity of a liquid crystal infiltrated photonic crystal fiber," *Photonics Technology Letters, IEEE*, vol. 23, pp. 408-410, 2011.

[20] S. Mathews, G. Farrell, and Y. Semenova, "Liquid crystal infiltrated photonic crystal fibers for electric field intensity measurements," *Applied optics*, vol. 50, pp. 2628-2635, 2011.

[21] A. Bozolan, R. M. Gerosa, C. J. De Matos, and M. A. Romero, "Temperature sensing using colloidal-core photonic crystal fiber," *Sensors Journal, IEEE*, vol. 12, pp. 195-200, 2012.

[22] L.Rindrof and O.Bang , "Sensitivety of photonic crystal fiber grating sensors bio sensing ,refractive index ,strain and temperature sensing " ,Department of communications , Technical university of Denmark ,Optical society of America 2013.

[23] Ashwini.M,P.Sharan,Srinivas.T," Temperature sensor based on photonic crystal fiber gratings ",applied photonics Lab,May2013.

[24] R. Wang, J. Yao, Y. Miao, Y. Lu, D. Xu, N. Luan, *et al.*, "A reflective photonic crystal fiber temperature sensor probe based on infiltration with liquid mixtures," *Sensors*, vol. 13, pp. 7916-7925, 2013.

[25] J. E. Antonio-Lopez, Z. S. Eznaveh, P. LiKamWa, A. Schülzgen, and R. Amezcua-Correa, "Multicore fiber sensor for high-temperature applications up to 1000 C," *Optics letters*, vol. 39, pp. 4309-4312, 2014.

[26] M. M. Tefelska, T. R. Woliński, S. Ertman, K. Mileńko, R. Łączkowski, A. Siarkowska, *et al.*, "Electric Field Sensing With Photonic Liquid Crystal Fibers Based on Micro-Electrodes Systems," *Journal of Lightwave Technology*, vol. 33, pp. 2405-2411, 2015.

[27] C. Markos, A. Stefani, and O. Bang, "Thermally tunable bandgaps in a hybrid As2S3/silica photonic crystal fiber," in *International Conference on Optical Fibre Sensors (OFS24)*, 2015, pp. 96343G-96343G-4.

[28] M. O. Ko, S.-J. Kim, J.-H. Kim, B. W. Lee, and M. Y. Jeon, "Electric field sensor based on cholesteric liquid crystal Fabry-Perot etalon," in *International Conference on Optical Fibre Sensors (OFS24)*, 2015, pp. 96345S-96345S-4.

[29] T. Wolinski, K. Szaniawska, K. Bondarczuk, P. Lesiak, A. Domanski, R. Dabrowski, *et al.*, "Propagation properties of photonic crystal fibers filled with nematic liquid crystals," *Optoelectronics Review*, vol. 13, p. 177, 2005.

[30] [30] E. Yablonovitch, "Air-filled fibres could speed up the Web," *Physics world*, vol. 12, p. 20, 1999.

[31] [31] B. Zsigri, C. Peucheret, M. D. Nielsen, and P. Jeppesen, "Transmission over 5.6 km large effective area and low-loss (1.7 dB/km) photonic crystal fibre," *Electronics Letters,* vol. 39, p. 1, 2003.

[32] T.Ritari,"Novel Sensor and telecommunication applications of photonic crystal fibers", 2006.

[33] W. Jin, J. Ju, H. L. Ho, Y. L. Hoo, and A. Zhang, "Photonic crystal fibers, devices, and applications," *Frontiers of Optoelectronics,* vol. 6, pp. 3-24, 2013.

[34] J. Limpert, T. Schreiber, S. Nolte, H. Zellmer, A. Tünnermann, R. Iliew, *et al.*, "High-power air-clad large-mode-area photonic crystal fiber laser," *Optics Express,* vol. 11, pp. 818-823, 2003.

[35] F. Benabid, J. C. Knight, G. Antonopoulos, and P. S. J. Russell, "Stimulated Raman scattering in hydrogen-filled hollow-core photonic crystal fiber," *Science,* vol. 298, pp. 399-402, 2002.

[36] A. M. Pinto and M. Lopez-Amo, "Photonic crystal fibers for sensing applications," *Journal of Sensors,* vol. 2012, 2012.

[37] G. Antonopoulos, *Super-enhanced stimulated Raman scattering and particle guidance in hollow-core photonic crystal fibres*, 2006.

[38] M. Ziemienczuk, "Coherent Gas-Laser Interactions via Stimulated Raman Scattering in Hollow-Core Photonic Crystal Fibers," 2012.

[39] N. Litchinitser, A. Abeeluck, C. Headley, and B. Eggleton, "Antiresonant reflecting photonic crystal optical waveguides," *Optics Letters,* vol. 27, pp. 1592-1594, 2002.

[40] R. Amezcua-Correa, "Development of hollow-core photonic bandgap fibres free of surface modes," University of Southampton, 2009.

[41] H.T.Salloom,"photonic crystal fiber sensors:modeling and application",PhD thesis,2014.

[42] K. Yoshida, Y. Furui, S. Sentsui, and T. Kuroha, "Loss factors in optical fibres," *Optical and Quantum Electronics,* vol. 13, pp. 85-89, 1981.

[43] K. Nagayama, M. Kakui, M. Matsui, T. Saitoh, and Y. Chigusa, "Ultra-low-loss (0.1484 dB/km) pure silica core fibre and extension of transmission distance," *Electronics Letters*, vol. 38, p. 1, 2002.

[44] OFS Furukawa Company, “Understanding fiber optic attenuation”, 2007.

[45] N. Massa,” Fundamental of Photonics Fiber Optic Telecommunication”, 2000.

[46] I. Gris Sanchez, "Fabrication and Applications of Low OH Photonic Crystal Fibres," University of Bath, 2012.

[47] V. Finazzi, T. M. Monro, and D. J. Richardson, "The role of confinement loss in highly nonlinear silica holey fibers," *Photonics Technology Letters, IEEE*, vol. 15, pp. 1246-1248, 2003.

[48] J. Vijay and M. Sabir, "Low-Flattened Dispersion Hexagonal Photonic Crystal Fiber With Low Confinement Loss," *International Journal of Emerging Technology and Advanced Engineering*, vol. 3, pp. 153-158, 2013.

[49] J. C. Baggett, T. M. Monro, K. Furusawa, V. Finazzi, and D. Richardson, "Understanding bending losses in holey optical fibers," *Optics Communications*, vol. 227, pp. 317-335, 2003.

[50] M. Nielsen, N. Mortensen, M. Albertsen, J. Folkenberg, A. Bjarklev, and D. Bonacinni, "Predicting macrobending loss for large-mode area photonic crystal fibers," *Optics express*, vol. 12, pp. 1775-1779, 2004.

[51] J. M. López-Higuera, L. Rodriguez Cobo, A. Q. Incera, and L. R. Cobo, "Fiber optic sensors in structural health monitoring," *Lightwave Technology, Journal of*, vol. 29, pp. 587-608, 2011.

[52] B. Culshaw, "Fiber optics in sensing and measurement," *Selected Topics in Quantum Electronics, IEEE Journal of*, vol. 6, pp. 1014-1021, 2000.

[53] W. J. Smith, *Modern optical engineering*: Tata McGraw-Hill Education, 1966.

[54] H. Y. Choi, M. J. Kim, and B. H. Lee, "All-fiber Mach-Zehnder type interferometers formed in photonic crystal fiber," *Optics Express,* vol. 15, pp. 5711-5720, 2007.

[55] A. N. Bashkatov and E. A. Genina, "Water refractive index in dependence on temperature and wavelength: a simple approximation," in *Saratov Fall Meeting 2002: Optical Technologies in Biophysics and Medicine IV,* 2003, pp. 393-395.

[56] A. A. O. M. Abdul–Karim and J. M. Abdul–Ammer, "Calculations Of Refractive Index For (MBBA) Liquid Crystal Material At Different Temperatures."

Appendix

LMA-10

Single-mode 10 µm core fiber

Single Mode Large Mode-area

- Low fiber loss from 500 to 1700 nm
- Single-mode at all wavelengths
- Radiation hard pure silica fiber
- Wavelength independent MFD

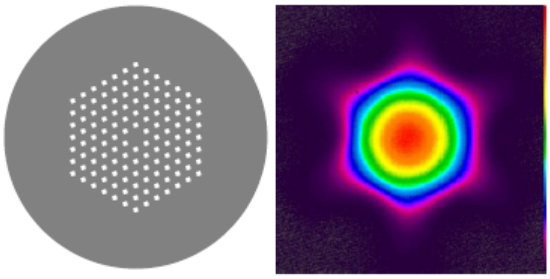

This single-mode photonic crystal fiber is optimized to exhibit low loss across the widest possible wavelength region from 500 nm to above 1700 nm while keeping an almost constant mode field diameter.

The fiber is endlessly single-mode with no higher order mode cut-off and delivers excellent mode quality at all wavelengths.

The fiber has a standard 125 µm outer diameter and is compatible with all common fiber tools.

This product is also available in a polarization-maintaining version as the LMA-PM-10.

Optical properties	
Single mode cut-off wavelength*	None
Attenuation @ 532 nm**	< 40 dB/km
Attenuation @ 632 nm**	< 20 dB/km
Attenuation @ 1064 nm**	< 5 dB/km
Mode field diameter @ 532 nm (1/e²)	8.4 ± 1.0 µm
Mode field diameter @ 1064 nm (1/e²)	8.8 ± 1.0 µm
NA @ 1064 nm (5%)	0.11 ± 0.02
Physical properties	
Core diameter	10.1 ± 0.5 µm
Outer cladding diameter, OD	125 ± 2 µm
Coating diameter	245 ± 10 µm
Core and cladding material	Pure silica
Coating material, single layer	Acrylate
Coating-Cladding concent. error	< 10 µm
Proof test level	0.5 %

Standard interfacing options	
FC/PC connector	0.0 ± 0.5 deg angle
FC/APC connector	8.0 ± 0.5 deg angle
Collapse and cleave	0.0 ± 0.5 deg angle

All interfaces are provided with a 150 ± 25 µm sealing length of the PCF structure.

Please contact us for other custom interfacing options.

* TIA-455-80-C standard ** 16 cm bend diameter

Applications

- Single-mode high power delivery
- Mode filtering
- Single-mode pigtailing

Typical spectral attenuation and dispersion

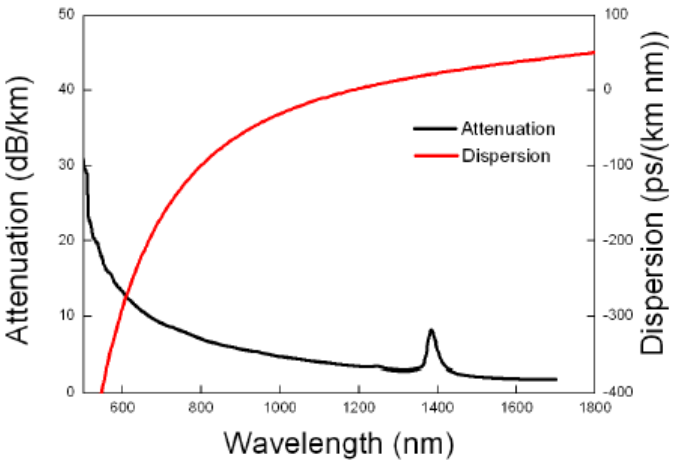

Typical MFD and NA

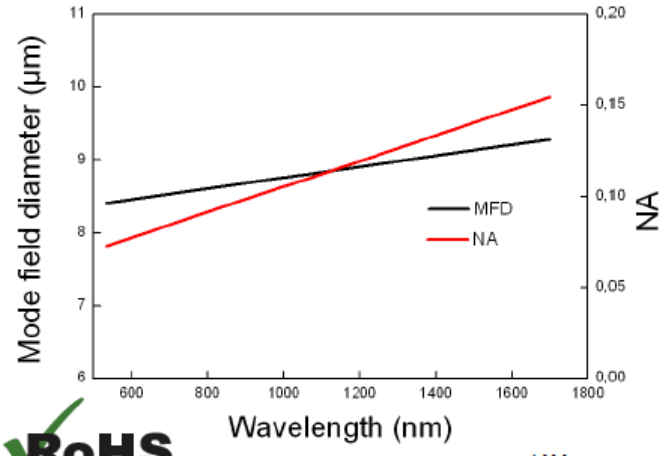

RoHS 2002/95/EC

LMA-10-v1--131104

NKT Photonics A/S (Headquarters)
Blokken 84 • 3460 Birkerød • Denmark
Phone: +45 4348 3900
Fax: +45 4348 3901
www.nktphotonics.com

NKT Photonics GmbH
Schanzenstrasse 39 • Bldg D9-D13
51063 Cologne • Germany
Phone: +49 221 99511-0
Fax: +49 221 99511-650

NKT Photonics Inc.
1400 Campus Drive West • Morganville
NJ 07751 • USA
Phone: +1 732 972 9937
Fax: +1 732 414 4094

الملخص

ان العمل الحالي يهدف الى استعمال الالياف البلورية الضوئية لتصميم متحسسات حرارة ومجال كهربائي بخصائص تصنيع مطلوبة تتضمن: حساسية عالية، اعادة التصنيع، وكلفة اقل من خلال الحقن بسائل خيطي (Nematic) بلوري من نوع (EBBA). ان الجديد في هذا العمل هو استخدام مادة EBBA والتي تتصف بقدرتها على اصطفاف جزيئاتها عند تعرضها الى مجال كهربائي خارجي، الامر الذي يجعلها تمتلك صفات البلورات أحادية المحور وتكون مفيدة في تطبيقات مختلفة.

تم تصميم وتنفيذ متحسسي الحرارة والمجال الكهربائي المقترحين، حيث ان عملية التصميم قد تطلبت المرور بطورين من العمل هما: طور تحضير السائل البلوري وطور تصميم المتحسسين. ان طور التحضير مسؤول عن تحضير مادة EBBA بأستخدام مكوناتها الكيميائية ليتم حقنها في الليف الضوئي البلوري في مراحل عمل قادمة وذلك بعد التأكد من جودتها. ومن اجل التحقق من جودة المادة المصنعة، تم استخدام مطياف تحويل فوريرللاشعة تحت الحمراء (FTIR) لتحديد طيف الانبعاث عند مدى درجات حرارة ٣٦-٨٠ درجة مئوية، وكذلك تم قياس مقادير معامل الانكسار لهذه المادة عند مدى درجات حرارة ٢٥-٨٠ درجة مئوية، حيث أظهرت النتائج ان معامل الانكسار يقل بزيادة درجات الحرارة. بعد ذلك، تم استخدام المادة EBBA في تصميم المتحسسين المقصودين. في حين ان طور تصميم المتحسس مسؤولا عن بناء المتحسس وضبط مكوناته بالشكل المطلوب.

تم تنفيذ المتحسس الحراري بربط قطعة صغيرة من ليف بلوري ضوئي نوع (LMA-10) مع ليف نمط وحيد تقليدي نوع (SMF-28) من طرف واستخدم رابط حر الحركة من الطرف الاخر. ثم أستخدم ليزر ثنائي بأطوال موجية (٨٥٠،١٠٦٠،١٥٥٠ *nm*) اضافة الى ليزر الهيليوم نيون بطول موجي (٦٣٢.٨*nm*) كمصادر ضوء واستخدم محلل طيف ضوئي عالي الحساسية (OSA) لمشاهدة وتسجيل طيف الانبعاث. في حين تم تنفيذ متحسس المجال الكهربائي باستخدام قطعة صغيرة ليف بلوري ضوئي ذو جوف فارغ من نوع (HC-1550) واستخدام ليزر ثنائي بطول موجي٦٥٠*nm* كمصدر ضوء يتم توجيهه من احد اطراف الليف في حين يملأ الطرف الاخر بمادة EBBA بواسطة ظاهرة الانابيب الشعرية، ومن ثم يتم تسجيل طيف الانبعاث بواسطة مطياف الالياف البصرية.

تم اختبار المتحسسات المقترحة وذلك بملأ ثقوب الهواء لليف الضوئي البلوري بالسائل البلوري بدلاً من الهواء. ولغرض تحسس الحرارة، تم تحضير مادة السائل البلوري EBBA وزجها في فراغات الليف البلوري الضوئي مملوء الجوف من النوع (LMA-10) والتي ادت

الى تغير معامل انكسار الليف البلوري الضوئي وأثرت ايضاً على نفاذية الليزر بداخله، يأتي هذا التأثير بسبب تغير معامل انكسار السائل البلوري. أظهرت النتائج ان قدرة طيف الانبعاث بعد ملأ الليف تزداد بزيادة درجات الحرارة. وأن اعلى حساسية تم استحصالها كانت $0.02 dBm/^oC$ عند طول موجي $1550 nm$ بسبب قلة ضياع الضوء و وهنه. وكذلك في متحسس المجال الكهربائي، تم ملأ فراغات الهواء بمادة السائل البلوري EBBA في ليف بلوري ضوئي نوع (HC-1550) لأرتفاع بحدود $1cm$. أظهرت النتائج ان قدرة الانبعاث لا تتغير حتى وصول شدة المجال الكهربائي الى $97.2 Vrms/mm$، وان المتحسس الكهربائي يعمل في منطقة مابين $97.2 Vrms/mm$ الى $146.8 Vrms/mm$ وبعدها يثبت مرة ثانية وان حساسية المتحسس الى ($0.00123 dBm.mm/Vrms$) عند الطول الموجي $650 nm$. ان مقادير الحساسية المستحصلة تعتبر مقبولة بالمقارنة ما تم ذكره في ادبيات سابقة، وهذا يؤكد صحة سير مراحل العمل والنتائج.

جمهورية العراق
وزارة التعليم العالي والبحث العلمي
جامعة النهـــرين
كلـيـة الـعـلـــوم

تصميم متحسس ألياف ضوئية بلورية

رســـــالـــــة
مقدمه الى كلية العلوم في جامعة النهرين
كجزء من متطلبات نيل درجة الماجستير
في علـوم الـفيـزيــاء

مـــن قبـــل
ســـرور عـــلي مـــهدي الخفـــاجي
(بكالوريوس علوم فيزياء ٢٠١٣)

اشراف

أ.م.د. سهـــى موســـى خـورشـــيد الأوسـي

١٤٣٧ هجرية ٢٠١٦ ميلادية